

INFORMATION TO USERS

This manuscript has been reproduced from the microfilm master. UMI films the text directly from the original or copy submitted. Thus, some thesis and dissertation copies are in typewriter face, while others may be from any type of computer printer.

The quality of this reproduction is dependent upon the quality of the copy submitted. Broken or indistinct print, colored or poor quality illustrations and photographs, print bleedthrough, substandard margins, and improper alignment can adversely affect reproduction.

In the unlikely event that the author did not send UMI a complete manuscript and there are missing pages, these will be noted. Also, if unauthorized copyright material had to be removed, a note will indicate the deletion.

Oversize materials (e.g., maps, drawings, charts) are reproduced by sectioning the original, beginning at the upper left-hand corner and continuing from left to right in equal sections with small overlaps. Each original is also photographed in one exposure and is included in reduced form at the back of the book.

Photographs included in the original manuscript have been reproduced xerographically in this copy. Higher quality 6" x 9" black and white photographic prints are available for any photographs or illustrations appearing in this copy for an additional charge. Contact UMI directly to order.

U·M·I

University Microfilms International
A Bell & Howell Information Company
300 North Zeeb Road, Ann Arbor, MI 48106-1346 USA
313/761-4700 800/521-0600

Order Number 9136035

**Radiation and convection heat transfer in particle-laden fluid
flow**

Jones, Peter Douglas, Ph.D.

Rice University, 1991

U·M·I
300 N. Zeeb Rd.
Ann Arbor, MI 48106

RICE UNIVERSITY

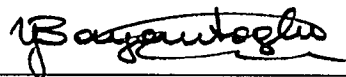
RADIATION AND CONVECTION HEAT TRANSFER
IN PARTICLE-LADEN FLUID FLOW

by

PETER DOUGLAS JONES

A THESIS SUBMITTED
IN PARTIAL FULFILLMENT OF THE
REQUIREMENTS FOR THE DEGREE
DOCTOR OF PHILOSOPHY

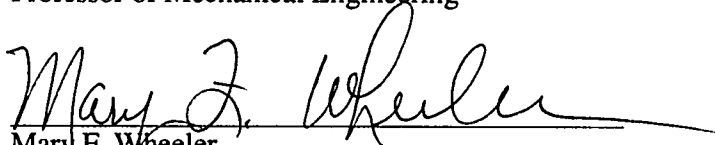
APPROVED, THESIS COMMITTEE



Yildiz Bayazitoglu, Director
Professor of Mechanical Engineering



Alan J. Chapman
Professor of Mechanical Engineering



Mary F. Wheeler
Noah Harding Professor of Mathematical Sciences

Houston, Texas

August, 1990

RADIATION AND CONVECTION HEAT TRANSFER IN PARTICLE-LADEN FLUID FLOW

by

Peter Douglas Jones

ABSTRACT

Combined radiation, convection, and conduction heat transfer are studied in a dispersed two phase flow of gray, laminar, axisymmetric media, where both phases are radiatively participating. The radiative transfer equation in curvilinear coordinates is coupled with an interpenetrating continua energy and momentum formulation for the two phase flow. The radiative transfer equation is set in a novel coordinate system which allows full variation of the radiation intensity in the plane of symmetry and expression of symmetric boundary conditions, without resort to the frequent assumption of azimuthal symmetry. The radiative transfer equation is solved using the discrete ordinates method, chosen for its relative accuracy and ability to numerically complement a differential energy formulation. An appropriate discrete ordinates quadrature is derived for the novel coordinate system.

The heat transfer model is used to study a proposed arrangement in which heated particles are seeded into heat exchange tubes running through a furnace in order to enhance heat transfer to a gas flowing in the tubes. It is found that with particles heated to temperatures approaching the furnace temperature, and mass loading ratios (seeded particle specific mass to carrying gas specific mass) up to the order of 10, significant enhancement in heat transfer to the gas is achieved. Such enhancement has the effect of reducing the required heat exchange tube length, thereby reducing the furnace size.

Interphase heat transfer between the dispersed particles and the semi-continuous gas is studied in detail by formally modeling combined radiation, conduction, and convection heat transfer between a particle and a semi-infinite medium. Results of this study demonstrate that in the seeding particle case, simple correlations for combined mode heat transfer are accurate. It is also found that the critical particle spacing at which interphase heat transfer is interfered with by neighboring particles is smaller for radiation dominated cases than for conduction dominated cases.

ACKNOWLEDGEMENT

Of the many who I must thank, there are just a few whose contribution has been vital in bringing this thesis out of the realm of dreams and into the light of completion. First, I am grateful to my wife, Elizabeth, who saw the dream before I did, had the vision to see that it was right, and had the tenacity and trust to see it through. There could be no greater inspiration than my advisor, Professor Yildiz Bayazitoglu, that consummate teacher of heat transfer, who knew when to save the day with a good idea, and also when to let me thrash it out for myself. No less important has been the steadfast support of the Department of Mechanical Engineering and Materials Science at Rice University, and its chairman, Professor J. Ed Akin. Finally, I take great pleasure in thanking my parents, Nancy F. and Dr. Paul S. Jones, whose lessons I am often slow to see, but find to be true nonetheless.

TABLE OF CONTENTS

Introduction

Enhanced heat transfer to gas flowing in ducts via particle seeding	1
Two phase flow models as applied to gas/particle flow	4
Radiation heat transfer in cylindrical media	6
Radiation heat transfer in particulate systems	10
Objectives	14

General Formulation

Interpenetrating continua model for dispersed gas/particle flow	16
Spatially axisymmetric directional coordinate system	22
Interphase heat transfer	25
Governing equations and boundary conditions	36

Numerical Solution Methodology

Discrete ordinates method	39
Quadrature	42
Discretized energy equations	45
Computational algorithm	46

Results and Discussion

Non-dimensional parameters	52
Verification	56
Behavior of a base case	57
Variation of individual parameters	61
Example calculation	70

Conclusions

References

Appendix A - Spatially axisymmetric directional coordinate system

Appendix B - Interphase heat transfer by combined radiation, conduction, and convection

APPENDIX A -

Spatially Axisymmetric Directional Coordinate System

<u>Introduction</u>	82
<u>Spatially Spherical Coordinates</u>	84
<u>Spatially Cylindrical Coordinates</u>	90

APPENDIX B -

Interphase Heat Transfer by Combined Radiation, Conduction, and Convection

<u>Introduction</u>	93
<u>Analysis</u>	
Governing equations	96
Coordinate system	97
Boundary conditions	97
Numerical procedure	99
<u>Results and Discussion</u>	102

LIST OF FIGURES

1. Gas heat exchange tube seeded with hot particles.	3
2. Coordinate system for combined radiation and convection in axisymmetric cylindrical coordinates.	26
3. Critical radius ratio, beyond which heat flux from black inner shell of a gray spherical annulus is within 5% of heat flux from a black sphere in an infinite medium, for $T_d/T_c=1.5$.	31
4. Combined radiation and conduction heat flux from a hot, black sphere in a gray infinite medium.	32
5. Combined radiation and conduction heat flux from a diffusely emitting and reflecting sphere in a gray infinite medium, with $T_d/T_c=1.5$.	33
6. Combined radiation and convection heat flux from a hot, black sphere in a gray infinite medium at low Peclet numbers, for $T_d/T_c=1.5$.	34
7. Computational algorithm	48
8. Temperature profiles at different cross-sections downstream for a gas/particle flow with the base case parameters.	58
9. Heat flux parameters as functions of downstream distance for a gas/particle flow with the base case parameters.	62
10. Heat exchange effectivity for the gas: all base case parameters constant except for mass loading ratio, M_L .	63
11. Heat exchange effectivity for the gas: all base case parameters constant except for tube to particle radius ratio, r^* .	65
12. Heat exchange effectivity for the gas: all base case parameters constant except for gas optical thickness, τ_c .	66
13. Heat exchange effectivity for the gas: all base case parameters constant except for conduction to radiation ratio, N_r .	67
14. Heat exchange effectivity for the gas: all base case parameters constant except for particle injection temperature, $\theta_{d,o}$.	68
15. Heat exchange effectivity for the gas: example case with no seeding particles, with $M_L=1$, and with $M_L=10$.	72
16. Heat exchange effectivity for the gas: example case comparison between present model and model neglecting radiative participation of the gas.	73

A.1. Spatially axisymmetric directional coordinate system for representation of radiation intensity in spatially spherical coordinates.	83
A.2 Correlation between differential spatial angles and differential directional angles - first kind.	86
A.3 Projection of spatial azimuthal differential angle ($d\psi$) on plane of directional polar differential angle ($d\alpha$).	87
A.4 Correlation between differential spatial angles and differential directional angles - second kind.	89
A.5 Spatially axisymmetric directional coordinate system for representation of radiation intensity in spatially cylindrical coordinates.	91
B.1 Spherical body in motion through a gray, absorbing, emitting, conducting medium.	95
B.2 Temperature profiles for a black sphere in an infinite medium; for radiation alone, conduction alone, and for combined radiation and conduction, with $T_d/T_c=1.5$ and $\kappa_d=1$.	105

INTRODUCTION

Enhanced Heat Transfer to Gas Flowing in Ducts via Particle Seeding

In instances where heat is transferred through the walls of a duct to a gas flowing in the duct, heat transfer to the gas may be enhanced if the gas is seeded with small particles, particularly if the particles are at a higher temperature than the gas. This effect is important in cases where gases, which have low heat carrying capacity, must be used in favor of high heat capacity liquids, due to high temperature or other practical constraints. A problem then exists in transferring as much heat as possible to the gas, in order to limit the necessary size of the heat transfer surfaces. Solving this problem by seeding the gas with particles has been proposed for general purposes (Gat, 1987), as well as for specific devices such as solar collectors (Hruby, et al, 1988).

In the case of gas flowing in a tube without particles, heat is transferred by convection from the hot tube walls to the cold gas. If the gas is radiatively participating, surface emission from the interior tube walls is also effective in heating the gas. The presence of particles contributes to heat transfer by a third mechanism: heat is transferred from the particles to the gas by radiation, conduction, and convection. In addition, heat is transferred directly from the walls to the particles by radiation, especially if the radiative absorption coefficient of the gas is low. This heat is then passed on to the gas from the heated particles.

In order to focus this study of combined mode heat transfer in gas/particle flows, an arrangement consisting of heat exchange tubes passing through a fluidized bed combustor is proposed. Fluidized bed combustors are the object of much current research due to their promise for efficient combustion of coal, and are characterized by high heat transfer to immersed surfaces (see Brewster and Tien, 1982b, Flamant and Menigault, 1987, Glicksman and Decker, 1982, Glicksman, et al, 1988, Goshayeshi,

et al, 1986, and Qian, et al, 1987, among others). The usual arrangement for extracting the heat of combustion is to pass heat exchange tubes directly through the combustor bed, which may be at a temperature on the order of 1000 K. Heat is transferred to a gas flowing in the tubes, from which it is then exchanged to a power generating loop, or used directly in a turbine or other device. Clearly, it is advantageous to transfer heat from the bed to the gas over as short a tube length as possible, in order to reduce the necessary combustion bed size and hence the amount of fuel burned in the bed. In order to enhance heat transfer to the gas, the flow is seeded with particles as illustrated in fig.1. These particles may be separated from the gas downstream of the combustion bed and re-injected upstream, possibly passing through the bed again for reheating.

The purpose of this study is to develop a model for calculating the heat transferred to a flowing gas seeded with hot particles. This model will serve both as a tool for comparative and absolute design studies, as well as serving as a framework for further refinements. Radiation heat transfer plays a primary role in high temperature combustors and in incident intensity cases such as an enhanced solar collector. However, radiation heat transfer calculations are particularly difficult, and efficient computational techniques for combined mode heat transfer are not yet fully developed. Therefore, the bulk of this research centers on radiative heat transfer methods which may be integrated with numerical methods for heat transfer by convection and conduction. As the gas and particles are not constrained to be either at the same temperature or flowing with the same velocity, the resulting model combines a radiative transfer formulation with a two phase flow momentum and energy formulation.

In addition to the direct applications of this research, there are also applications to more general areas of heat transfer in gas/particle flows. These areas are primarily associated with combustion; for instance: the thermal characteristics and propagation of solid combustion products; combustion of particulates such as ground coal (in the bed

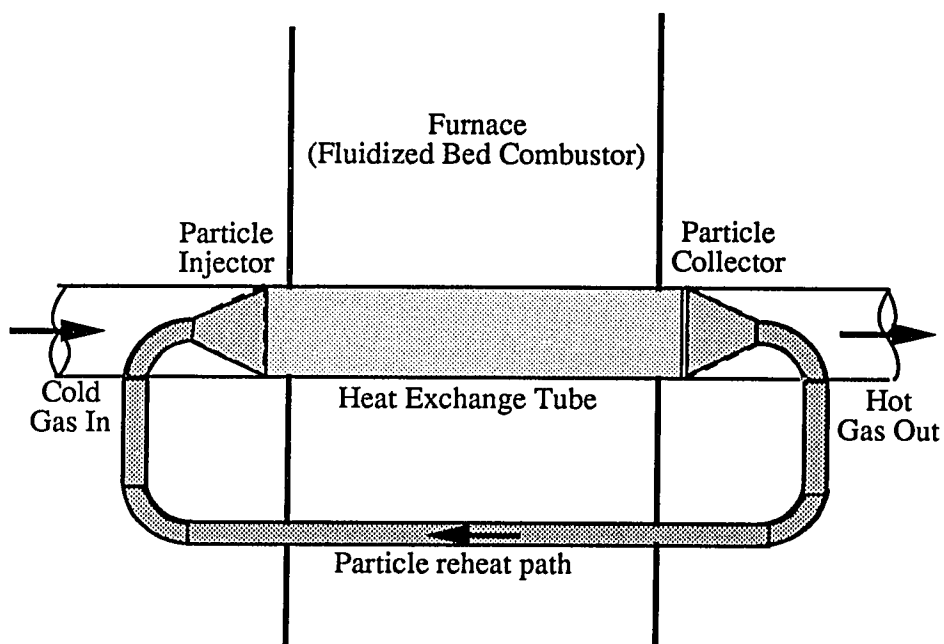


Figure 1 - Gas heat exchange tube seeded with hot particles

external to the tubes considered here); or the temperature and concentration distributions leading to dust explosions of volatile materials. Radiation, conduction/convection, and particle motion are important in each of these cases. In a review of current analytical techniques for radiation heat transfer in combustion systems, Viskanta and Menguc (1987) identified needs for improved numerical modeling of multi-dimensional radiation and combined mode heat transfer, and for improved modeling of interphase (gas/particle) temperature differences. This study attempts to address these needs.

Two Phase Flow Models as Applied to Gas/Particle Flow

In multiphase flow theory, an accepted general formulation (Boure and Delhay, 1982) is to write conservation equations for each distinct phase, and couple these equations through interphase transfer terms. Thus, for momentum, one would write a momentum equation for the gas, containing terms for momentum flux and rate of change, and including pressure, viscous, and external force terms. Similarly, the momentum equation for the particle phase might include external forces and the effects of particle collisions. The coupling interphase transfer term, for momentum exchange between the phases, would be drag on the particles. Momentum would be given up in the form of drag by the particles, and an equivalent momentum would be gained by the gas. For the energy formulation, the equations for each phase would include energy flux and rate of change, intraphase transfer terms such as conduction and heat generation, and an interphase term corresponding to the local heat exchange between the gas and the particles. An important conceptual feature of such formulations is that the local velocity and thermal boundary layers near each phase boundary are neglected. This is not so much that the phase boundary is considered to be a step change in velocity or temperature, but rather that the velocities and temperatures for each phase are considered to be local bulk properties which respond only in an averaged way to

micro-distributions of higher or lower value. The phases are coupled by the interphase transfer terms, which account for the physical presence of a boundary layer through the resulting flux of momentum or energy.

The situation considered here is a dispersed two phase flow, in which elements of a dispersed phase (particles) are widely separated within a continuous phase (gas). The dispersed assumption allows several simplifications in the general two phase flow formulation. In the energy formulation, conduction is represented by Fourier's law in the continuous phase, using the thermal conductivity of this phase unmodified by the presence of particles. Conduction in the dispersed phase is neglected, which denotes neglect of heat transfer in interparticle and particle/wall collisions. These assumptions are justified (Soo, 1989) for rigid particles separated by a mean of ten particle diameters, which is the nominal separation considered here. The particles are also considered to be of small Biot number, so that temperature non-uniformity across an individual particle may be neglected. The heat transfer mechanisms considered in this study are: conduction within the continuous phase and between the walls and the continuous phase; radiation within the combined continuous and discrete phases and between the walls and the combined phases; and combined radiation, conduction, and convection between the discrete and continuous phases.

Two overall approaches have been applied to dispersed two phase flow: the Lagrangian/ Eulerian and interpenetrating continua formulations. In the Lagrangian/Eulerian approach, the continuous phase is formulated as an Eulerian fluid, while the dispersed phase is modeled by a Lagrangian formulation for individual particles (Faeth, 1983). The computational approach is to solve the continuous phase without particles, use the continuous solution to predict particle behavior, and alternate between continuous and dispersed solutions until convergence is achieved. Generally, the dispersed solution is computed for representative particles, approximating the

dispersed phase to be made up of packets of similarly behaving particles. The Lagrangian/Eulerian formulation is particularly useful in large scale turbulent flows, such as free shear flows, where particle number density at the edge of the flow becomes very small.

The interpenetrating continua formulation treats the dispersed phase as pseudo-continuous, in that the number density (concentration) of particles is treated as a flow variable, and the dispersed phase is described in a compressible Eulerian sense (see Crowder, et al, 1984, Faeth, 1983, and Sharma and Crowe, 1979, Tien, 1961). This approach loses the accuracy of describing individual particle tracks and temperatures, but gains in relative computational simplicity by requiring simulation of two sets of continuous equations, as opposed to thousands of representative discrete sets. The interpenetrating continua formulation refers to the general two phase flow approach of mass, momentum, and energy conservation equations for each phase, interconnected (penetrated) by interphase transfer terms. This formulation is accurate for enclosed flows, and is used in this study for that reason.

Radiation Heat Transfer in Cylindrical Media

Radiation contributions to heat transfer are governed by the distribution of radiation intensity throughout the medium. The radiation intensity is the intensity of the infrared range electromagnetic waves emanating from all points in the medium and from its boundaries (walls). These waves are directional; thus, the radiation intensity is a quantity that varies with direction in addition to spatial location. This is fundamentally different than, for instance, the components of a vector. A vector is a single quantity which has magnitude and direction, both of which may vary with location. Thus, a vector is comprised of three components in three dimensional space: either a magnitude and two variables which define direction, or three orthogonal components. However,

intensity varies continuously with direction. Put another way, there is a unique radiation intensity for each of the infinite number of discrete directions at a single point in space. Heat flux by radiation is a vector, however. At a single point, the integral over all directions of the component of radiation intensity projected in a particular direction defines the radiation heat flux in that direction.

The radiation intensity is governed in a radiatively participating medium by the radiative transfer equation. This is an integro-differential equation which relates the change in intensity along an arbitrary differential path to: the intensity scattered out of the path; the intensity scattered into the path; the intensity absorbed along the path; and the intensity emitted by the medium along the path. The radiative transfer equation may be solved analytically only for very simple geometries, generally for geometries which vary with only one dimension in space and are azimuthally symmetric (and therefore one-dimensional in direction). Even for these geometries, the distribution function of the in-scattering term, which is an integral, might necessarily be restricted in order to allow solution. Often, analytical solutions to the radiative transfer equation depend upon special integral functions, whose value must be numerically simulated. Hence, many analytical solutions to the radiative transfer equation are ultimately numerical.

The present problem is expressed in cylindrical coordinates. Solution to the radiative transfer equation in cylindrical coordinates is much more challenging than in Cartesian coordinates; however, one-dimensional solutions have been derived using a variety of exact and approximate techniques. Many of these methods are reviewed by Howell (1988), in a general way. Heaslet and Warming (1966) have demonstrated an exact analysis based on the simplifying assumptions of spatial variation only in the radial direction, azimuthal symmetry, and isotropic scattering. Heaslet and Warming were able to reduce the radiative transfer equation from an integro-differential equation to an exact integral equation. This equation was transformed to an integral equation for

the radiation heat flux, combined with an energy equation with only radiation heat flux contributions, solved numerically for general cases, and solved analytically for special cases. Azad and Modest (1981a) derived a similar formulation which allows inclusion of conductive/convective modes of heat transfer.

Another approach to solution of the radiative transfer equation is to express the radiation intensity as a spherical harmonic series. In this method, also called P_N , the radiation intensity is expressed as a series of order N of Legendre polynomials of the cosine of the intensity's directional polar angle. The radiative transfer equation based on this approximation is a set of ordinary differential equations which are much simpler than the integral equation resulting from exact analysis. The P_N method has been applied to azimuthally symmetric cylindrical geometries by Bayazitoglu and Higenyi (1979) for higher order N 's, showing good accuracy as compared to Heaslet and Warming's results, and with considerably lower computational effort. Solution of the approximate equations may be achieved in closed form in simple cases (Bayazitoglu and Jones, 1990, Bayazitoglu and Suryanarayana, 1989).

An assumption common to these works on solution of the radiative transfer equation in cylindrical coordinates is that spatial variation is allowed only in the radial direction, and azimuthal symmetry is assumed in the directional variation, with the polar angle aligned in the radial direction. In this study, full axisymmetry is allowed for flow in the heat exchanger tube, with variation in axial and radial coordinates. This allows accurate representation of short tubes, in addition to allowing eventual application to combustion chambers, which are typically short. Exact (integral) analysis solutions to the radiative transfer equation are not available in multiple dimensions. Spherical harmonics solutions in multiple spatial dimensions and Cartesian coordinates are given by Ratzel and Howell (1982), and by Menguc and Viskanta (1985a), all at the cost of a considerable increase in complexity over spatially

single dimensioned problems. Further, due to a lack of boundary conditions for the directional partial derivative terms which appear in curvilinear expressions of the radiative transfer equation, these multi-dimensioned P_N formulations may not be rigorously applied to the present axisymmetric problem, regardless of one's willingness to contend with their computational complexity.

Having considered exact analysis brought to the point of numerical solution of an integral equation, and functional approximation brought to the point of numerical solution of a set of differential equations, a direct numerical solution of the radiative transfer equation is now considered. This is known as the method of discrete ordinates. The discrete ordinates method amounts to a finite difference representation of the radiative transfer equation in up to five dimensions (three spatial and two directional), where the directional mesh is a quadrature derived from some criteria, and each point in the directional mesh has an associated integration weight. One of the earliest workers to set out the discrete ordinates method was Chandrasekhar (1950), and the method was extensively developed in the 1960's by Carlson and Lathrop (see Carlson, 1970, Carlson and Lathrop, 1968) for application to neutron transport problems. The mathematical foundation of the discrete ordinates method is treated in several texts, notably Lewis and Miller (1984). More recent application to radiation heat transfer problems has come in papers by Fiveland (1984, 1987, 1988), Truelove (1987, 1988), Kumar, et al (1988), and Yucel, et al (1988), among others, who have addressed radiation problems in up to three dimensions in Cartesian media. Again, it is important to note that while in Cartesian geometries the directional terms appear only as parameters in the radiative transfer equation, in curvilinear coordinate systems the equation includes partial derivatives in the directional variables as well. This makes the application of the discrete ordinates method to curved coordinate systems considerably more complex than its application to Cartesian coordinate systems. Yucel and Williams

(1987, 1988) studied combined radiation and conduction in cylindrical media, although they made the assumption of azimuthal symmetry for the radiative transfer equation.

The radiative transfer equation is coupled through temperature to the energy conservation equation. Radiative transfer equation solutions, as they appear in the literature, are often given for a specified temperature profile or for an energy equilibrium accounting only for radiative transfer. By expressing a more complete energy equation, including conduction and convection effects within the medium, combined mode heat transfer problems may be solved (see Bayazitoglu and Jones, 1990, Chawla and Chan, 1980, Desoto, 1968, Harris, 1989, Lee and Buckius, 1986, Lee et al, 1988, Ratzel and Howell, 1982, Razzaque, et al, 1984, and Yener and Ozisik, 1986). The usual solution algorithm is to estimate temperature, solve the radiative transfer equation for this estimate, use the intensity solution to solve the energy equation, make a new temperature estimate from the result, and continue until convergence is achieved. Much of the attractiveness of the discrete ordinates method results from the ease with which it may be integrated into numerical solution algorithms for the energy equation (Howell, 1988).

In the foregoing discussion, the assumption of grayness has been made. Electromagnetic intensity is a quantity which varies with wave frequency, in addition to spatial location and direction. Grayness refers to the simplifying assumption that intensity is uniform with frequency. Gray solution methods may be generalized to non-gray cases using techniques which are analytically straightforward, but computer-intensive (see Ozisik, 1973, also Siegel and Howell, 1981).

Radiation Heat Transfer in Particulate Systems

Treatment of radiation heat transfer in particulate or gas/particle systems involves determination of: radiation properties of the medium; independence from the

geometrical arrangement of particles in the medium; and interphase heat transfer between the gas and particle phases.

In determining medium properties, particular concern has been directed toward scattering by non-spherical particles, and toward categorizing particle shape and size distributions in ground coal and coal combustion products (Buckius and Hwang, 1980, Menguc and Viskanta, 1985b). More general studies are directed toward liquid droplets and liquid fuel combustion products, as a means of calculating medium absorption as a function of pressure and radiation pathlength (Skocypec and Buckius, 1984, 1987, Goodwin and Ebert, 1987, Self, 1987). In the present study, the shape, distribution, and other properties of the seeding particles may be controlled. The seeding particles may be considered to be spherical, opaque, diffuse, and of known size distribution, in which case their radiative properties may be approximated simply, as described by Siegel and Howell (1981). However, application of the results of this study to noncontrolled media would require more careful consideration of irregular characteristics for the gas/particle medium.

In a dispersed two phase flow, intensity scattering may generally be assumed to be independent. In the study of packed and fluidized beds, it is recognized that in a packed or dense fluidized bed, a scattered ray will reflect off many other particles, and hence scattering for the medium is as much a function of particle arrangement as of the individual particle properties. For a dispersed particle field, however, the arrival of a scattered ray at a second scattering particle surface is a more random event, and overall scattering is independent, similar to scattering in a homogeneous material. Drolen and Tien (1987) have compared scattering models appropriate to either extreme in order to define a demarcation between independent and dependent scattering. Their results are given in terms of volume fraction of particles in the flow and the ratio of particle diameter to radiation wavelength. For particles of the size and concentrations

considered in the present study, Drolen and Tien define scattering to be clearly independent. Their work supports the experimental conclusions of Brewster and Tien (1982a).

In cases where interphase heat transfer is very rapid and interphase temperature differences are small, the gas/particle medium is often considered to be a single homogeneous phase. This is the case for very small particles, on the micron scale, especially when the initial temperatures of the phases are the same. Due to the fine particle sizes, studies of such cases tend to concentrate on turbulent particle transport and the effect on the total medium radiative properties of the distribution of particle number density and size (see Menguc and Viskanta, 1986, Modest, 1981, Smith, et al, 1987, Tabanfar and Modest, 1983, 1987).

In dispersed particle flows with significant interphase temperature difference, interphase heat transfer is generally approximated as the heat transfer between a particle of assumed shape and an infinite medium. In a medium where neither phase is radiatively participating, this heat transfer is simply the Nusselt number, which is well known for spherical particles. Sirignano (1983) presents results of a numerical convection study of one sphere aligned in the wake of a second sphere, and examines the effect on heat transfer from both spheres as a result of their interaction. At the low interphase Peclet numbers typical of particles in the millimeter and below size range, at separations on the order of ten diameters as considered here, even alignment directly in a wake does very little to change the heat transfer from that calculated for an infinite medium. Crowe (1979) has suggested a simple addition to the Nusselt number in cases where radiation is significant, consisting of the blackbody radiation between the particle surface and the local gas bulk temperature. This is only correct for an optically thin gas.

One of the earlier studies of radiation and conduction/convection heat transfer in

dispersed gas/particle flows with interphase temperature difference is reported by Echigo and Hasegawa (1972) and Echigo, et al (1972). This study employed an interpenetrating continua formulation with laminar flow and no interphase velocity interference (zero drag). The continuous phase was considered to be radiatively non-participating, with a high Peclet number based on the total flow (one-dimensional conduction). An exponential integral solution for the radiation heat flux was used with negligible axial variation and no scattering. Interphase heat transfer, as appropriate for a non-participating continuous phase, was by conduction/convection alone. Inlet temperatures for mixture flow in a tube were equal. By varying the mass loading ratio of the dispersed phase to the continuous phase, the optical thickness of the dispersed phase, and the conduction to radiation ratio, temperature profiles were computed with a finite difference scheme. The phases were found to develop little temperature difference. The effect of the particles on the heat transfer at the walls of the tube was found to be very significant, especially at very low conduction to radiation ratios. Azad and Modest (1981a) produced a similar analysis, with the addition of flow turbulence and linear radiation scattering. Forward scattering was shown to increase heat transfer at the tube walls.

In a major study sponsored by the U.S. Department of Energy, Smith, et al (1981, 1985) developed a model for ground coal combustion in cylindrical combustion chambers. Their model employed a turbulent, Lagrangian/Eulerian formulation for detailed study of particle motion. Radiation was represented by a four-flux model for intensity, using linearly anisotropic scattering and participation by both phases. Multi-flux methods were examined by Brewster and Tien (1982b) for plane parallel media, and found to be reasonably accurate for optically thin media and isotropic scattering. Multi-flux methods are less accurate in cylindrical media. Smith, et al used Crowe's (1979) radiative addition to conductive/convective interphase heat transfer.

This model is weak in many details of radiation heat transfer, as Smith, et al sought primarily to study combustion's chemical effects. Lee and Humphrey (1986) produced a similar model, oriented more particularly toward particle transport in pipelines, which employs only a two-flux radiation model. Lee and Humphreys noted the effect on dispersed and continuous phase temperature profiles of the augmented heat source/sink action of the particles which results from an accounting for radiation.

Objectives

The objectives of the present work are to study heat transfer to a radiatively participating gas flowing in a tube with hot walls and injected with particles with interphase differences in temperature and velocity. The goal of such study is to determine techniques and parameters for enhancing heat transfer to the gas. As compared to previous studies which established models which might be used to study these phenomena, improvements will be offered in the area of interphase heat transfer between the particles and gas, and in the area of overall radiation heat transfer modeling.

When both phases are radiatively participating, current interphase heat transfer techniques accounting for radiation heat transfer ignore the combined mode nature of this phenomenon by simply summing a conductive/convective correlation with a radiative correlation. A combined analysis must be performed to determine the total heat flux resulting from the combined temperature profile in the thermal boundary layer around an individual particle. This analysis will yield the heat transfer correlation information to more accurately express combined mode interphase heat transfer. This will help to meet the need, noted by Viskanta and Menguc (1987), for more accurate assessment of interphase temperature differences in gas/particle flows.

Improved radiation heat transfer methods are needed by the current models

which could be used to study these phenomena (Echigo, et al, 1972, Azad and Modest, 1981a, Smith, et al, 1985). More accurate radiation heat transfer methods are available, and have been applied to single or homogeneous phase cylindrical problems, although they have not been extended to cases of arbitrary (nonlinear) scattering and axial intensity variation. Howell (1988) has pointed out the flexibility and simplicity of the discrete ordinates method for use in combined mode heat transfer problems. However, this method has not been extended to problems without azimuthal symmetry in spatial curvilinear coordinate problems. This extension will be made in order to accurately express combined mode heat transfer in the fully axisymmetric problem of gas/particle flow in cylinders of finite length.

It should be emphasized that the present analysis assumes a gray medium. Most practical applications of this analysis involve media which are particularly non-gray. The objective of this paper is to outline an analytical technique for solving combined energy/intensity problems in axisymmetric cylindrical media. However, practically applicable results of this analysis must await a computationally intensive but analytically straightforward extension to non-gray media. Furthermore, it should be noted that the intent of this analysis is to focus on aspects of heat transfer, and on radiation heat transfer in particular. Therefore, the present study has been limited to laminar flow. Using the following formulation, the methods of this study could easily incorporate a turbulent or otherwise more sophisticated flow model.

GENERAL FORMULATION

Interpenetrating Continua Model for Dispersed Gas/Particle Flow

The general formulation used in this study allows one-dimensional flow in a circular duct with two phases: a widely dispersed particle phase and a nearly continuous gas phase. The phases may have unequal velocities, and these velocities may also vary across the duct. Momentum exchange is by fluid dynamic drag on the particles, where each particle is unaffected by any other particle (Sirignano, 1983), and collisions between walls and particles and between particles are assumed to be random and of short duration, and therefore their effect is neglected (Soo, 1967). The continuity equations for the two phases are:

$$\frac{\partial}{\partial x} \left[\rho_c \left(1 - \frac{4}{3} \pi r_d^3 N \right) u_c \right] = 0 \quad (1a)$$

for the continuous phase, where x is the tube axial coordinate, ρ_c is the continuous phase density, r_d is the particle radius, assumed constant in this study, N is the particle number density, and u_c is the local continuous phase velocity; and:

$$\frac{\partial}{\partial x} \left(\rho_d \frac{4}{3} \pi r_d^3 N u_d \right) = 0 \quad (1b)$$

for the dispersed phase, where ρ_d is the dispersed phase material density and u_d is the local dispersed phase velocity. Equation 1b reduces to:

$$\frac{\partial}{\partial x} (N u_d) = 0 \quad (1c)$$

For this dispersed gas/particle flow, a low volume fraction of particles is assumed, so

that:

$$1 \gg \frac{4}{3} \pi r_d^3 N \quad (2)$$

We also assume that ρ_c is constant, with the result that eq.1a reduces to:

$$\frac{\partial u_c}{\partial x} = 0 \quad (3a)$$

so u_c is assumed unchanged from its initial distribution, for which we impose the fully developed laminar profile:

$$u_c(r) = 2U_c \left[1 - \left(\frac{r}{R} \right)^2 \right] \quad (3b)$$

where U_c is the mean continuous phase velocity and r is the radial coordinate in the tube, and R is the tube radius.

The assumption is made that although the continuous phase has an effect on the momentum of the dispersed phase, the particles are not numerous enough to significantly affect the bulk continuous phase momentum. The equation for momentum conservation in the dispersed phase is:

$$\rho_d \frac{4}{3} \pi r_d^3 N \frac{du_d}{dt} = N \frac{1}{2} C_D (\pi r_d^2) \rho_c (u_c - u_d)^2 \quad (4a)$$

Where the assumption is made that the Reynolds number based on the particle radius and the relative interphase velocity is less than 1, so for Stoke's flow:

$$C_D = \frac{24}{Re} = \frac{24 \mu_c}{2 r_d \rho_c (u_c - u_d)} \quad (4b)$$

where μ_c is the continuous phase viscosity. Equation 4a may be simplified using eq.4b

to give:

$$u_d \frac{\partial u_d}{\partial x} = \frac{\mu_c}{32 \rho_d r_d^2} (u_c - u_d) \quad (4c)$$

With an initial condition:

$$u_d(r, x=0) = f_u^o u_c(r) \quad (5)$$

where f_u is the local ratio between the dispersed phase and continuous phase velocities, and f_u^o is its initial value, the two phase velocity field is completely described. Note that gravity and other body forces have been neglected, implying that the particles are small and primarily carried along with the flow.

Energy conservation is expressed similarly to the formulations of Tien (1961), Echigo, et al (1972), and Smith, et al (1981). Neglecting heat generation by combustion or other reactions, the continuous phase energy equation is:

$$\left(\rho c_p \right)_c \frac{DT_c}{Dt} + \left(\nabla \cdot q^C \right)_c + \left(\nabla \cdot q^R \right)_c = q_{cd} \quad (6a)$$

where c_{pc} is the continuous phase specific heat, T_c is the local continuous phase bulk temperature, q^C is conduction heat flux through the continuous phase, q^R is radiation heat flux through the two phase medium, q_{cd} is the local interphase heat transfer by combined radiation, conduction, and convection, and the substantial derivative form is employed. The dispersed phase energy equation is expressed:

$$\left(\rho c_p \frac{4}{3} \pi r_d^3 N \right)_d \frac{DT_d}{Dt} + \left(\nabla \cdot q^R \right)_d = -q_{cd} \quad (6b)$$

where c_p is the dispersed phase specific heat and T_d is the local particle temperature.

Small Biot number is assumed, so that T_d may be taken to be constant over the individual particle (Bayazitoglu and Ozisik, 1988). Note that the right side of eq.6a, which is the heat given to the continuous phase by the dispersed phase, is the opposite of the corresponding term in eq.6b, so that the sum of eqs.6 is the total energy equation for the gas/particle mixture. The effect of the dispersed phase on conduction through the continuous phase is neglected, and Fourier's law is assumed:

$$\left(\nabla \cdot \mathbf{q}^C \right)_c = -k \nabla^2 T_c \quad (7)$$

where k is the thermal conductivity of the continuous phase. The usual substitution for the radiation heat flux gradient for gray media, when combining radiative transfer with an energy formulation, is (Ozisik, 1973):

$$\left(\nabla \cdot \mathbf{q}^R \right) = 4\pi\kappa B - \kappa \int_0^\pi \int_0^{2\pi} I \sin \alpha \, d\gamma \, d\alpha \quad (8a)$$

which is derived from the radiative transfer equation, discussed below. B is the blackbody term:

$$B = \frac{\sigma_b}{\pi} T^4 \quad (8b)$$

where σ_b is Boltzmann's constant, κ is the absorption coefficient of the medium, and the index of refraction has been assumed to be 1. The angular terms in eq.8a may be understood to imply integration over the entire unit directional sphere, and the specific directional coordinate system will be described later. I is the radiation intensity, a function of all spatial and directional coordinates. The radiation intensity is taken to be common to the total two phase medium. However, its heating effects must be distributed into the distinct phases. Note that κ is a coefficient for the entire right hand

side of eq.8a. The total absorption coefficient for the gas/particle medium is the sum of the absorption coefficients for the individual phases. Therefore, the suggestion of Smith, et al (1981) is followed in order to distribute the heat flux gradient from the intensity into the energy relations for the two phases:

$$\left(\nabla \bullet \mathbf{q}^R \right)_c = 4\pi\kappa_c B_c - \kappa_c \int_0^\pi \int_0^{2\pi} I \sin \alpha \, d\gamma \, d\alpha \quad (8c)$$

$$\left(\nabla \bullet \mathbf{q}^R \right)_d = 4\pi\kappa_d B_d - \kappa_d \int_0^\pi \int_0^{2\pi} I \sin \alpha \, d\gamma \, d\alpha \quad (8d)$$

In this formulation, buoyancy effects are neglected so that the energy equations are uncoupled from the momentum and continuity equations. Thus, the continuous and dispersed phase velocity fields and the particle number density may be solved independently of the phase temperatures, and the velocity results may be used directly in the energy equations.

The radiation intensity is solved as a single quantity, as opposed to considering the intensity to be separated between phases. A useful visualization is that the intensity exists primarily within the continuous phase, which is an absorbing, emitting, non-scattering gas. The particles dispersed within the gas are then considered to be point absorbers, emitters, and scatterers of radiation. Hence, variations in radiation intensity within each individual particle are not considered. Radiation intensity is governed by the integro-differential radiative transfer equation for gray media, expressed after Smith, et al (1981):

$$\frac{dI}{ds} + (\kappa_c + \kappa_d + \sigma_d)I = \kappa_c B_c + \kappa_d B_d + \frac{\sigma_d}{4\pi} \int_0^\pi \int_0^{2\pi} p(\alpha, \gamma, \tilde{\alpha}, \tilde{\gamma}) I(\tilde{\alpha}, \tilde{\gamma}) \sin \tilde{\alpha} \, d\tilde{\gamma} \, d\tilde{\alpha} \quad (9)$$

where ds is a differential pathlength expressed in a spatial-directional coordinate system, σ_d is the scattering coefficient due to the dispersed phase, and p is a scattering function, integrated over all angles which scatter into a single direction. Scattering in any medium is generally a function of particles distributed in that medium. Since in this case the pure gas and the particles are considered separately, there is no scattering coefficient associated with the gas alone. Also note the separation of the blackbody term into dispersed phase and continuous phase contributions.

For solution, the differential pathlength ds must be expanded into its scalar components for a spatially axisymmetric, cylindrical coordinate system:

$$\frac{dI}{ds} = \frac{dr}{ds} \frac{\partial I}{\partial r} + \frac{dx}{ds} \frac{\partial I}{\partial x} + \frac{d\alpha}{ds} \frac{\partial I}{\partial \alpha} + \frac{d\gamma}{ds} \frac{\partial I}{\partial \gamma} \quad (10)$$

In Cartesian coordinate representations, the coefficients of the directional partial derivatives ($d\alpha/ds$, $d\gamma/ds$) are zero. However, in curvilinear coordinates (spherical and cylindrical), these are nonzero, and hence it is necessary to have directional boundary conditions in order to solve the angular partial derivatives. This issue will be addressed later in more detail.

For a dispersion of particles, radiative properties may be expressed (Buckius and Hwang, 1980, Menguc and Viskanta, 1985b, Ozisik, 1973):

$$\kappa_d = \pi r_d^2 N Q_a \quad (11a)$$

$$\sigma_d = \pi r_d^2 N Q_s \quad (11b)$$

where Q_a and Q_s are termed absorption and scattering efficiencies, respectively. As the particles seeded into the tube are of controlled size, shape, material, and initial concentration, the conditions of Siegel and Howell (1981) may be met, in which for

spherical, diffuse, opaque, and disperse particles, which are large compared to the wavelength of radiation (wavelength parameter x about 5 or more, particle volume fraction of about 10^{-3}). These assumptions allow the following:

$$Q_a = \epsilon_d \quad (12a)$$

$$Q_s = 1 - \epsilon_d \quad (12b)$$

where ϵ_d is the surface emissivity of the particle material. For a diffuse, opaque spherical particle, the scattering function may be calculated rigorously as (Siegel and Howell, 1981):

$$p(\theta) = \frac{8}{3\pi} (\sin \theta - \theta \cos \theta) \quad (13a)$$

where θ is the scattering angle:

$$\cos \theta = \cos \alpha \cos \bar{\alpha} + \sin \alpha \sin \bar{\alpha} \cos(\gamma - \bar{\gamma}) \quad (13b)$$

Equation 13a strongly favors backscattering from individual particles.

Spatially Axisymmetric Directional Coordinate System

At a given point in space, the direction of radiation intensity is defined by a location on a unit sphere which is centered at that point in space. To imagine the effect of the geometry of the unit directional sphere, it is helpful to make analogy to location on the surface of the earth, were the earth of unit radius. This location is defined by two independent angles, a polar angle and an azimuthal angle. The polar angle is measured relative to a defined polar axis, analogous to the earth's axis through the north and south poles. The polar angle would then be analogous to latitude, with a

range from $-\pi/2$ to $\pi/2$. The azimuthal angle refers to rotation about the polar axis, analogous to longitude, and has a range from 0 to 2π . In the coordinate system used in eqs.8, 9, and 10, α is the latitude (although its range has been transformed to 0 to π), and γ is the longitude.

The directional portion of a spatial directional coordinate system generally moves, changing origin and orientation, with the spatial location. Imagine the spatial location of the center of the earth defined in a coordinate system based on the center of the sun. Further imagine radiative intensity to be analogous to any property in space, say electromagnetic flux. Expressing the electromagnetic flux at any point on earth in a solar system based coordinate system (or the value of radiation intensity in the analogous problem considered here) would then depend upon the location of the center of the earth in a sun-centered spatial coordinate system, and also on the point's location on the earth's surface relative to the spatial coordinate system. In a similar way, expression of radiation intensity requires location in a spatial coordinate system, and specification of a direction at that spatial location.

In most expressions of the radiative transfer equation, the directional portion of the spatial-directional coordinate system is based on a polar axis which is instantaneously aligned with the radial vector in the spatial portion of the coordinate system (Ozisik, 1973, Viskanta and Menguc, 1987). In other words, for most published solutions of the radiative transfer equation, the direction of the radiation intensity is taken relative to an axis which is an extension of the line from the origin (the center of the sun) to the spatial location (the center of the earth). (This represents divergence from the earth-sun example, as the earth's polar axis is roughly perpendicular to the radial vector). Generally, azimuthal symmetry is assumed

(invariance with relative longitude). The polar boundary condition then results, either explicitly stated or implicitly included in a functional approximation (Menguc and Viskanta, 1986), that the intensity's partial derivative with respect to polar angle (relative latitude) is zero at the polar axis (now aligned with the earth-sun radial vector), regardless of the azimuthal angle. This symmetry condition is crucial to earlier solutions of the radiative transfer equation in curvilinear coordinates. For a one spatial dimension problem, the azimuthal symmetry assumption is quite justified.

In a spatially axisymmetric problem, rather than one which is radially symmetric, symmetry is relative to a plane hinged along the axis of symmetry. The zero slope condition only applies to path variations, ds , which are normal to this plane of symmetry. If the polar axis which defines the directional coordinate system is an extension of the radial vector, then that axis lies in the plane of symmetry. In such a case, the zero slope condition will only hold as a polar partial derivative boundary condition for azimuthal directions which are normal to the plane. In other words, the zero slope condition becomes a function of two variables, polar and azimuthal angle, rather than one. Therefore, the zero slope condition fails to function as a partial derivative boundary condition for the traditional spatial directional coordinate system (polar axis as a radial extension) when applied to fully axisymmetric problems.

In order to regain the use of the zero slope condition as a single variable boundary condition, it is necessary to employ a directional coordinate system in which paths normal to the plane of symmetry, at the plane of symmetry, are excursions in one variable. Such a coordinate system, designated the Spatially Axisymmetric Directional coordinate system, is derived in Appendix A. In this coordinate system, the polar axis is oriented normal to the plane of symmetry. When the polar angle is such that the direction lies in the plane of symmetry, excursion normal to the plane of symmetry is a function only of the polar angle, α , and not of the azimuthal angle, γ . Therefore, the

zero slope condition may be applied as a partial derivative boundary condition in the polar angle, α , at the point where $\alpha=\pi/2$. The axisymmetric problem is directionally symmetric about the spatial plane of symmetry, in addition to spatially symmetric.

Therefore, only the range $0 \leq \alpha \leq \pi/2$ must be solved. Using the Spatially Axisymmetric Directional coordinate system in the cylindrical spatial coordinates of the present problem, we may express the intensity pathlength derivative (see Appendix A):

$$\frac{dI}{ds} = \frac{1}{r} \sin \alpha \cos \gamma \frac{\partial}{\partial r} (Ir) - \sin \alpha \sin \gamma \frac{\partial I}{\partial x} + \frac{1}{r} \cos \gamma \frac{\partial}{\partial \alpha} (I \cos \alpha) \quad (14)$$

Note that the azimuthal partial derivative (γ) is not used in spatially cylindrical coordinates, as $d\gamma/ds=0$ uniquely.

The complete Spatially Axisymmetric Directional coordinate system as applied to spatially cylindrical media is illustrated in fig.2

Interphase Heat Transfer

One reason for using the interpenetrating continua model is to avoid solving the microstructure of temperature and velocity detail surrounding each particle in a gas/particle flow. As regards temperature, of course there can physically be only one temperature at a single point. If that point is in the gas, then this temperature is T_c . If the point is on a particle, then the temperature is T_d . If the point is in the gas but close to the particle, then the temperature is in the thermal boundary layer of the particle. An essential assumption of the interpenetrating media model is that only the bulk phase temperatures T_c and T_d are treated, and the thermal boundary layer, the transition zone between the dispersed and continuous phases, is neglected. This is a computational

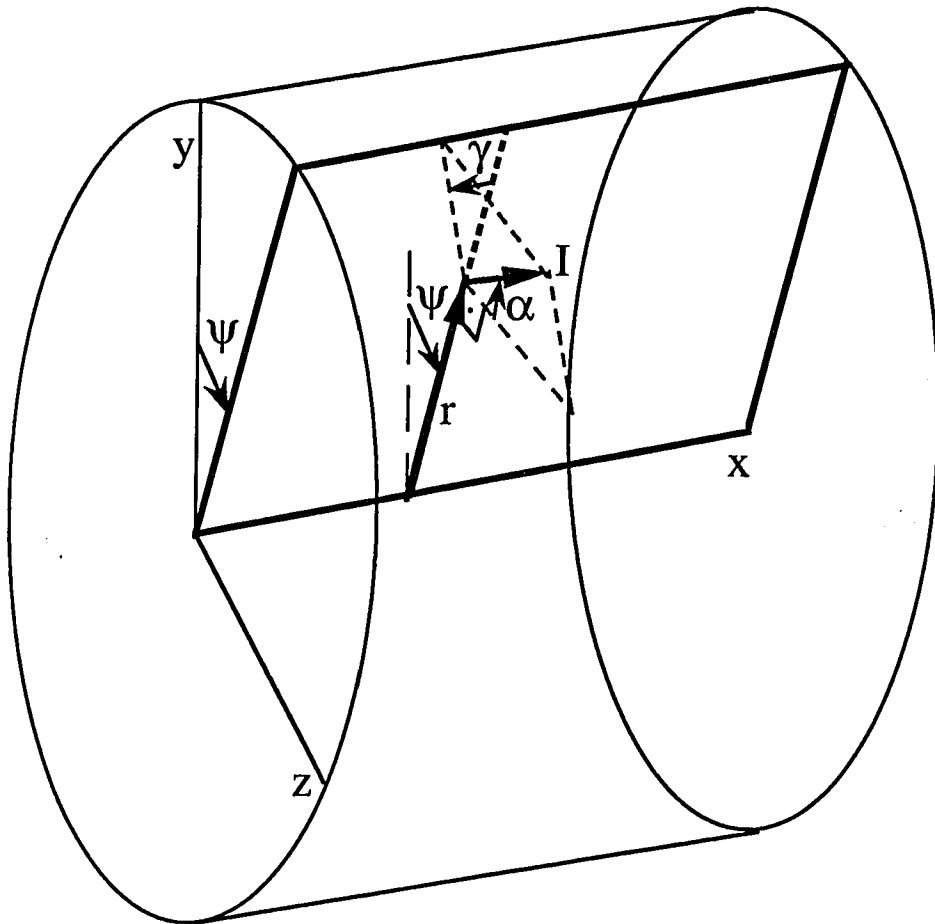


Figure 2 - Coordinate system for combined radiation and convection heat transfer in axisymmetric cylindrical coordinates

device, necessary because with dispersed phase concentrations up to the order of tens of billions (1×10^{11}) per cubic meter, it could never be possible to model the details of each thermal boundary layer.

Still, those boundary layers exist. The thermal gradient in the boundary layer gives rise to a heat flux from the particle to the gas nearby, which the gas spreads within itself by its own heat transfer mechanisms to elevate the local bulk temperature of the continuous phase. Hence, the particles act as heat sources (or sinks) distributed throughout the continuous phase. The particles have their own initial temperature and heat storage capability, which acts to meter out heat to the gas. In cases of low radiative participation by the gas, the particles even have a mechanism (radiation) for receiving heat directly from the duct walls, and then passing it on to the gas. Thus, a crucial element in modeling a gas/particle flow is accurate expression of the heat exchange between the particle and gas phases.

In radiatively non-participating gases, the interphase heat transfer mechanism is only by conduction and convection. In this case, it is common (Faeth, 1983) to use conduction/convection correlations for a single sphere (if this is an approximately correct shape) in an infinite medium. The medium surrounding a single particle is not infinite, of course, but for small particles, say less than 1mm diameter, separated from other particles by ten diameters on the average, the approximation is fairly good (Sirignano, 1983). (Most dispersed gas/particle flows meet this level of separation, while most fluidized beds, for instance, do not).

The infinite medium conduction/convection correlations are derived by writing an energy equation in a spherical annulus between the constant temperature sphere surface and a constant temperature outer boundary. This is the diffusion equation in the case of conduction (Bayazitoglu and Ozisik, 1989). The equation is solved with the outer boundary expanded to infinity. The heat flux result is non-dimensionalized by the

temperature difference between the sphere and the outer boundary. In dispersed two phase flow, this temperature difference is the temperature difference between the constant temperature particle (low Biot number), or more precisely the local bulk temperature of the dispersed phase, and the local bulk temperature of the continuous phase. For the low interphase Peclet numbers typical of gas/particle flows, where the Peclet number is derived from the very small particle diameter and the very low interphase velocity difference, the interphase heat flux is expressed by the Nusselt number correlation (Clift, et al, 1978):

$$Nu = \frac{2r_d q_{cd}}{k(T_d - T_c)} = 1 + (1 + Pe)^{1/3} \quad (15)$$

where Nu is the Nusselt number, and Pe is the Peclet number, $Pe = RePr$ (Reynolds number times Prandtl number), or $Pe = 2r_d(u_d - u_c)(\rho c_p)_c/k$. Although the flow field from which eq.15 is derived is only strictly accurate up to $Re=1$ ($Re = 2r_d(u_d - u_c)\rho_c/\mu_c$, $Pr \approx 0.7$), eq.15 gives a fairly accurate description of Nu up to $Pe=10$ (Clift, et al, 1978).

In cases where radiation from the particles is important as well, Crowe (1979) has suggested the following correction:

$$q_{cd} = Nu \frac{k(T_d - T_c)}{2r_d} + \epsilon_d \sigma_b (T_d^4 - T_c^4) \quad (16)$$

This can only be correct in gases where κ_c is not too large, because as the gas becomes more radiatively participating, the temperature profile in the particle boundary layer is altered from the diffusion equation solution, and eq.15 no longer holds (to say nothing of the second term on the right hand side of eq.16, which expresses radiation heat

transfer).

In order to find a heat transfer correlation between a spherical particle and the surrounding gas where radiation, conduction, and convection are all significant, an analysis analogous to that which produced eq.15 was carried out, as described in Appendix B. In this analysis, a combined mode energy equation, similar to eq.6a, was written in a spherical annulus between a particle and an outer boundary. The annular medium was considered to be absorbing, emitting, conducting, and in low Re motion. As noted above, scattering is a feature of interparticle radiative transfer, hence the pure gas annulus considered for the purpose of calculating heat transfer between the gas and the particles is considered to be non-scattering. The equation was solved by methods similar to those described in the following sections. As an outer boundary condition, the continuous medium was considered to radiate a blackbody intensity at the bulk temperature of the gas toward the particle. The thickness of the annulus was extended until the magnitude of the heat flux leaving the particle ceased to change significantly, and this heat flux was considered to be the infinite medium result. It is interesting to note that the annular thickness required to achieve infinite medium results is considerably less in the cases where radiation is a greater part of the total heat flux. Figure 3 demonstrates the necessary annular thickness as a function of the parameter $\kappa_c r_d$ for a range of Planck numbers, Pl ($Pl = k/4r_d\sigma_b T_d^3$, high Pl for mostly conduction heat transfer, low Pl for mostly radiation heat transfer). The results of this study were non-dimensionalized by a composite of radiation and conduction terms, in order to provide regular movement between mostly radiating cases and mostly conducting cases. Thus:

$$q_{cd} = q_{cd} \left[\sigma_b (T_d^4 - T_c^4) + \frac{k}{2r_d} (T_d - T_c) \right] \quad (17)$$

where q_{cd}' is a function of Pl , $\kappa_c r_d$, ϵ_d , T_d/T_c , and Pe . Results for $\epsilon_d = 1$ and $Pe = 0$ are shown in fig.4. Results for a range of ϵ_d are shown in fig.5, and for a range of Pe in fig.6. In fig.6, note that the effect of convection is reduced in cases with more significant radiation heat flux contribution. Comparing eq.16 to figs.4 and 5, it is found that for small $\kappa_c r_d$, less than about 0.1, eq.16 is reasonably accurate. However, eq.16 has no capacity for variation with $\kappa_c r_d$, and so eq.16 results in overestimates of the interphase heat transfer rate as $\kappa_c r_d$ is increased.

For purposes of automating the study of heat transfer in the whole gas/particle mixture, q_{cd}' was fit with the following approximation:

$$q_{cd}' = \left\{ a + b \tanh \left[c \log(\kappa_c r_d) + d \right] \right\} \frac{e}{2} \left[1 + (1 + f g Pe)^{1/3} \right] \quad (18a)$$

where:

$$a = 1.5633 + 0.6850 \log(Pl) - 0.4245 \frac{T_c}{T_d} \text{sech} [0.4796 - 1.4565 \log(Pl)]$$

$$0.5 \leq a \leq 1.92 \quad (18b)$$

$$b = -0.14 + 0.21 \log(Pl) + \frac{T_c}{T_d} (-0.1511 - 0.0111 Pl)$$

$$-0.5 \leq b \leq -0.05 \quad (18c)$$

$$c = 2 \quad (18d)$$

$$d = -0.05 + 0.15 \log(Pl) \quad (18e)$$

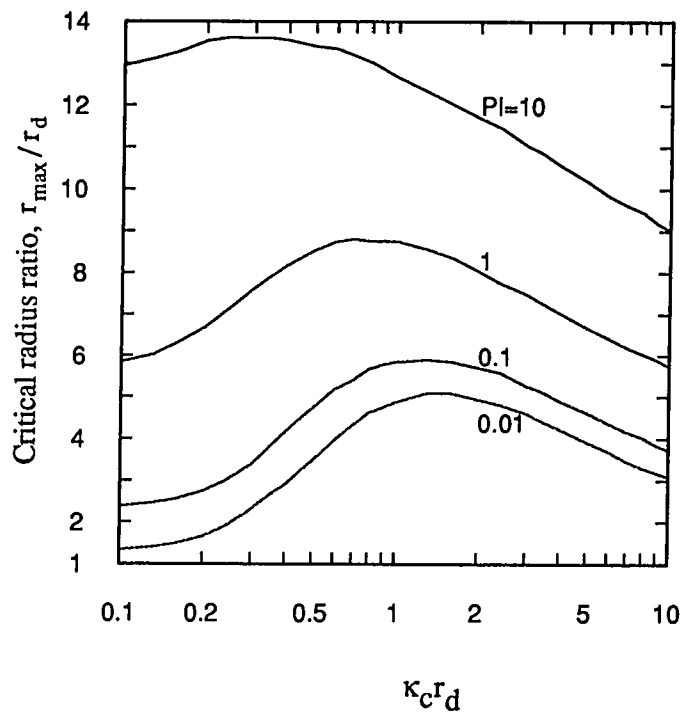


Figure 3 - Critical radius ratio, beyond which heat flux from black inner shell of a gray spherical annulus is within 5% of heat flux from a black sphere in a gray infinite medium, for $T_d/T_c = 1.5$.

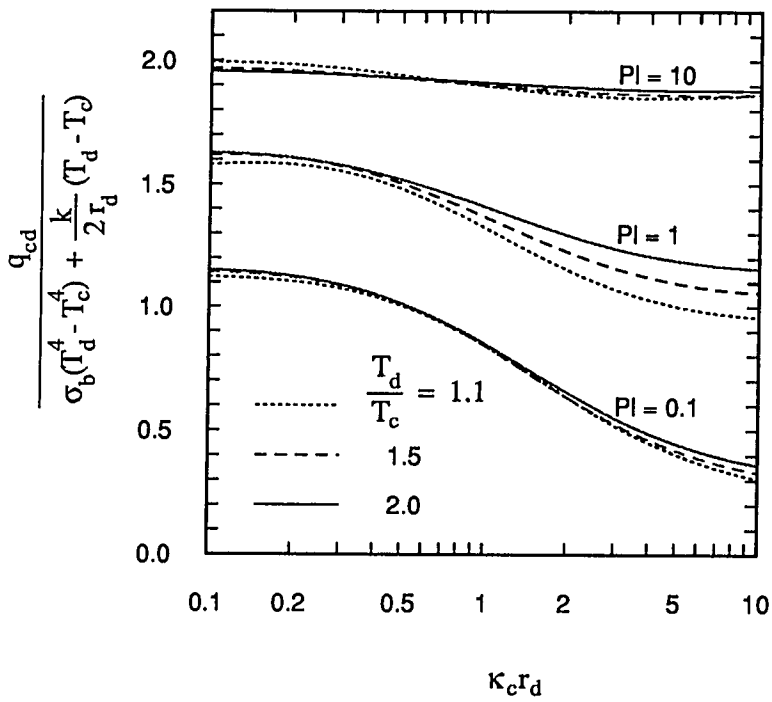


Figure 4 - Combined radiation and conduction heat flux from a hot, black sphere in a gray infinite medium.

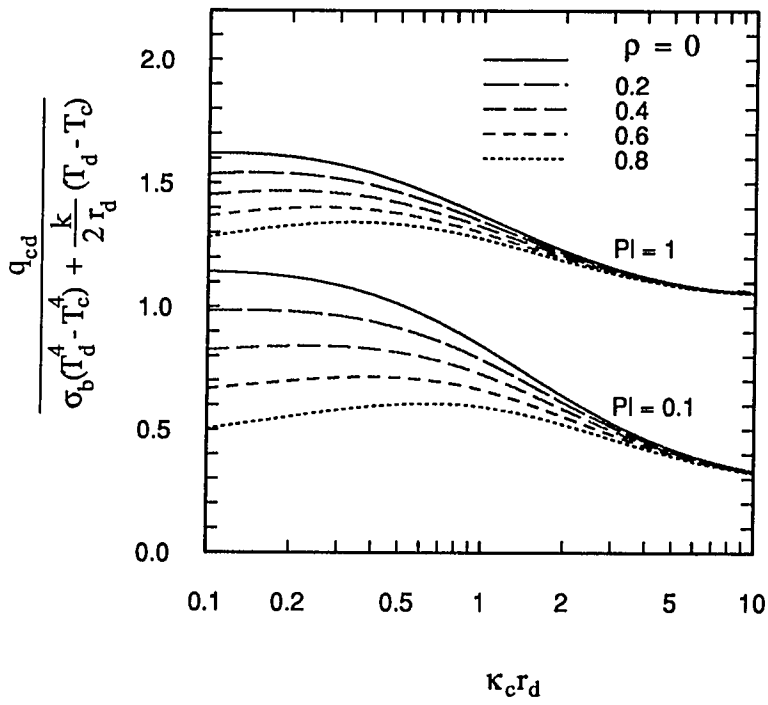


Figure 5 - Combined radiation and conduction heat flux from a diffusely emitting and reflecting sphere in an infinite gray medium, with $T_d/T_c = 1.5$.

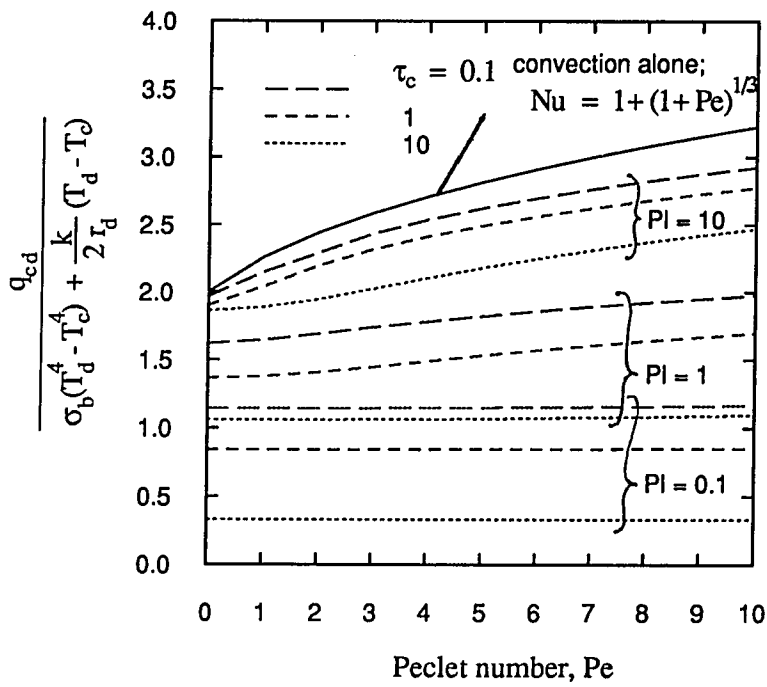


Figure 6 - Combined radiation and convection heat flux from a hot, black sphere in a gray, infinite medium at low Peclet numbers, for $T_d/T_c = 1.5$.

$$e = 1 - 0.08 (1 - \epsilon_d) Pl^{0.65} \left\{ 1 - \tanh \left[\log(\kappa_c r_d) \right] \right\} \quad (18f)$$

$$f = \frac{1}{2} \left[1 - \tanh \left(1.0651 - 0.7196 \log(Pl) \right) \right] \quad (18g)$$

$$g = 1 - \tanh \left(1.3336 \log(\kappa_c r_d) \right) \quad (18h)$$

Equations 18 provide a reasonably accurate fit of the data in figs.4, 5, and 6; however, caution should be used in applying these equations, as they were derived for a gray medium.

It should be emphasized that the effort in Appendix B to determine q_{cd} is not an attempt to calculate the detailed micro-distribution of radiation intensity within a dispersed gas/particle system. This would be analogous to attempting to calculate the exact temperature at all points within the local thermal boundary layers around each individual particle, abandoning the assumptions of the interpenetrating continua approximation. Further, the goal of Appendix B is not to quantify the entire exchange of radiation between the tube boundaries and the particle, or between the particles themselves. These exchanges are accounted for by the system radiative transfer equation for the entire dispersed two phase flow. What is attempted is to calculate an exchange of heat between a single particle and the surrounding gas, so that interphase heat transfer may be treated by an approximation which accounts for radiation in addition to convection and conduction. This heat exchange may not be calculated by simply adding pure radiation results to pure convection results because heat transfer in either mode depends on the detailed distribution of temperature in the thermal boundary layer. Inclusion of additional modes modifies this distribution, and makes correlations for either mode alone invalid in a combined mode setting. Therefore, in order to estimate the heat transfer between a particle and the surrounding gas, a single,

isothermal sphere in motion through a conducting, absorbing, emitting, non-scattering fluid is analyzed in Appendix B at a given far field temperature.

Governing Equations and Boundary Conditions

With the coordinate system for radiative transfer and the interphase heat transfer terms complete, the governing energy equations may be written in scalar form. Expanding eq.6a into scalar form, using eqs.7, 8b, 8c, and 17, and neglecting transience, the continuous phase energy equation is written:

$$\begin{aligned} (\rho c_p u)_c \frac{\partial T_c}{\partial x} - k \left[\frac{1}{r} \frac{\partial}{\partial r} \left(r \frac{\partial T_c}{\partial r} \right) + \frac{\partial^2 T_c}{\partial x^2} \right] + 4\kappa_c \sigma_b T_c^4 - \kappa_c \int_0^\pi \int_0^{2\pi} I \sin \alpha \, d\gamma \, d\alpha \\ = q_{cd}' 4\pi r_d^2 N \left[\sigma_b (T_d^4 - T_c^4) + \frac{k}{2r_d} (T_d - T_c) \right] \end{aligned} \quad (19a)$$

where q_{cd}' may be defined by eqs.18 or through a look-up table based on figs.4, 5, and 6. Expanding eq.6b by using eqs.8b, 8d, 11, 12, and 17, the dispersed phase energy equation is written:

$$\begin{aligned} (\rho c_p u)_d \frac{r_d}{3} \frac{\partial T_d}{\partial x} + \epsilon_d \sigma_b T_d^4 - \frac{\epsilon_d}{4} \int_0^\pi \int_0^{2\pi} I \sin \alpha \, d\gamma \, d\alpha \\ = q_{cd}' \left[\sigma_b (T_d^4 - T_c^4) + \frac{k}{2r_d} (T_d - T_c) \right] \end{aligned} \quad (19b)$$

The velocity fields represented in eqs.19 may be solved completely with eqs.3b, 3c, 4c, and 5. Equations 19 are solved using the methods described below, with the initial conditions:

$$T_c(r, x=0) = T_c^o \quad (20a)$$

$$T_d(r, x=0) = T_d^o \quad (20b)$$

and the boundary condition:

$$T_c(r=R, x) = T_w \quad (21)$$

where T_w is the tube wall temperature, which might be taken to be the combustion bed temperature. The constant temperature boundary condition of eq.21 suggests a high level of heat transfer from the combustion bed exterior to the tube. This may be reasonable considering the relatively high heat transfer coefficients typically transmitted to such tubes (Goshayeshi, et al, 1986) in comparison to heat transfer to a gas flowing through the tube's interior.

The radiative transfer equation, eq.9, may be combined with eqs.11, 12, 13, and 14 to form:

$$\begin{aligned} & \frac{1}{r} \sin \alpha \cos \gamma \frac{\partial}{\partial r} (Ir) - \sin \alpha \sin \gamma \frac{\partial I}{\partial x} + \frac{1}{r} \cos \gamma \frac{\partial}{\partial \alpha} (I \cos \alpha) + (\kappa_c + \pi r_d^2 N) I \\ &= (1 - \epsilon_d) \frac{r_d^2 N}{4} \int_0^\pi \int_0^{2\pi} p(\alpha, \gamma, \tilde{\alpha}, \tilde{\gamma}) I(\tilde{\alpha}, \tilde{\gamma}) \sin \tilde{\alpha} d\tilde{\gamma} d\tilde{\alpha} \\ &+ \kappa_c \frac{\sigma_b}{\pi} T_c^4 + \epsilon_d r_d^2 N \sigma_b T_d^4 \end{aligned} \quad (22)$$

The boundary conditions for radiation intensity are:

$$\frac{\partial I(r, x, \alpha=\pi/2, \gamma)}{\partial \alpha} = 0 \quad (23a)$$

representing directional axisymmetry,

$$\frac{\partial I(r=0, x, \alpha, \gamma)}{\partial r} = 0 \quad (23b)$$

representing spatial axisymmetry, and

$$\begin{aligned}
I\left(r=R, x, \alpha, \frac{\pi}{2} \leq \gamma \leq \frac{3\pi}{2}\right) &= \epsilon_w \frac{\sigma_b}{\pi} T_w^4 \\
+ \frac{(1 - \epsilon_w)}{\pi} \int_0^\pi \left[\int_0^{\pi/2} + \int_{3\pi/2}^{2\pi} \right] I \sin^2 \alpha \cos \gamma \, d\gamma \, d\alpha & \quad (23c)
\end{aligned}$$

which represents diffuse emission and reflection from the tube walls. The integral over γ in eq.23c is split, as $0 \leq \gamma \leq \pi/2$ and $3\pi/2 \leq \gamma \leq 2\pi$ face toward the tube wall, while $\pi/2 \leq \gamma \leq 3\pi/2$ faces away from the wall.

NUMERICAL SOLUTION METHODOLOGY

Discrete Ordinates Method

The radiative transfer equation is solved using the method of discrete ordinates (Carlson and Lathrop, 1968, Duderstadt and Martin, 1978, Lewis and Miller, 1984, Fiveland, 1984, 1987, 1988). This is an entirely numerical method in which the radiative transfer equation is integrated over a differential cell of spatial volume and directional solid angle. The cell intensity is then solved over the computational mesh using a marching solution algorithm. The integral scattering term is estimated prior to solution, updated after solution, and iteratively updated until it has converged. The spatial mesh is chosen to suit the problem, both for the energy equations and the radiative transfer equation. The directional mesh, however, is chosen to suit a quadrature. Resulting from that quadrature are the directional mesh points (the ordinates) and associated integration weights. In this formulation, the suggestion of Abu-Shumays (1977) is applied to split the integration weights at a single ordinate point

(α_p, γ_m) : $w_{lm} = w_l w_m$. In applying the discrete ordinates method to curvilinear coordinates, the partial derivatives for the directional angles must be treated specially. This will be illustrated by the discretized form of the radiative transfer equation.

Multiplying by a differential element of volume, $(2\pi r dr)(dx)(\sin\alpha d\alpha)(d\gamma)$, integrating over the ranges $r_{j-1/2}$ to $r_{j+1/2}$ and $x_{k-1/2}$ to $x_{k+1/2}$, and recognizing that the integral of

$(\sin\alpha d\alpha)(d\gamma)$ over a cell about an ordinate (α_p, γ_m) is w_{lm} , results approximately in:

$$\begin{aligned}
& 2\pi (x_{k+1/2} - x_{k-1/2}) \sin \alpha_\ell w_\ell \cos \gamma_m w_m \left[I_{j+1/2, k, \ell, m} r_{j+1/2} - I_{j-1/2, k, \ell, m} r_{j-1/2} \right] \\
& - \pi (r_{j+1/2}^2 - r_{j-1/2}^2) \sin \alpha_\ell w_\ell \sin \gamma_m w_m \left[I_{j, k+1/2, \ell, m} - I_{j, k-1/2, \ell, m} \right] \\
& + 2\pi (r_{j+1/2} - r_{j-1/2})(x_{k+1/2} - x_{k-1/2}) \cos \gamma_m w_m \left[I_{j, k, \ell+1/2, m} A_{\ell+1/2} - I_{j, k, \ell-1/2, m} A_{\ell-1/2} \right] \\
& + (\kappa_c + \pi r_d^2 N) \pi (r_{j+1/2}^2 - r_{j-1/2}^2)(x_{k+1/2} - x_{k-1/2}) w_\ell w_m I_{j, k, \ell, m} \\
& = \sigma_b \pi (r_{j+1/2}^2 - r_{j-1/2}^2)(x_{k+1/2} - x_{k-1/2}) w_\ell w_m \left(\frac{\kappa_c}{\pi} T_c^4 + \epsilon_d r_d^2 N T_d^4 \right) \\
& + \frac{\pi}{2} (1 - \epsilon_d) r_d^2 N (r_{j+1/2}^2 - r_{j-1/2}^2)(x_{k+1/2} - x_{k-1/2}) w_\ell w_m \sum_{\ell=1}^L \sum_{m=1}^M p_{\ell, m, \ell, m} I_{j, k, \ell, m} w_\ell w_m \quad (24)
\end{aligned}$$

Note that in the scattering term, summing to $\ell=L$ corresponds to half of the α range, $0 \leq \alpha \leq \pi/2$, as only half of the range $0 \leq \alpha \leq \pi$ need be considered due to symmetry. In eq.24 some approximations have been made in the α integrations in order to retain the relative simplicity of the ordinate and weight interactions. In order to retain the balance of the equation, the coefficients inside the brackets in the $\partial I / \partial \alpha$ term (third line of eq.24) have been altered. The criterion is applied that for I equal to a constant, dI/ds should be zero (Carlson and Lathrop, 1968, Duderstadt and Martin, 1978, Lewis and Miller, 1984; in other words, for constant I , the first three lines of eq.24 should sum to zero). This results in a recursion equation for these altered coefficients:

$$-\sin \alpha_\ell w_\ell = A_{\ell+1/2} - A_{\ell-1/2} \quad (25)$$

By analogy to the analytical coefficient in eq.14, $\cos \alpha$, the recursion is started with a value $A_{L+1/2}=0$, where $\alpha_{L+1/2}=\pi/2$, the angle just beyond the last ordinate point, and the recursion of eq.25 proceeds backwards in ℓ . This stratagem (use of balanced coefficients) is found to be vital to the numerical stability of eq.24.

Equation 14, the radiative transfer equation, is a first order equation in several

variables. As a consequence, only single point boundary values may be considered in a general numerical solution; i.e., marching methods must be employed. In order to improve the accuracy of this scheme, the linear cell assumption is employed (an extension of the technique of Carlson and Lathrop, 1968, Duderstadt and Martin, 1978, and Lewis and Miller, 1984):

$$I_{j,k,\ell,m} = w_j^+ I_{j+1/2,k,\ell,m} + w_j^- I_{j-1/2,k,\ell,m} \quad (26a)$$

$$I_{j,k,\ell,m} = w_k^+ I_{j,k+1/2,\ell,m} + w_k^- I_{j,k-1/2,\ell,m} \quad (26b)$$

$$I_{j,k,\ell,m} = w_\ell^+ I_{j,k,\ell+1/2,m} + w_\ell^- I_{j,k,\ell-1/2,m} \quad (26c)$$

where, for instance:

$$w_j^+ = \frac{r_j - r_{j-1/2}}{r_{j+1/2} - r_{j-1/2}} \quad (27a)$$

$$w_j^- = \frac{r_{j+1/2} - r_j}{r_{j+1/2} - r_{j-1/2}} \quad (27b)$$

and the intermediate mesh points are evenly spaced:

$$r_{j+1/2} = \frac{1}{2}(r_{j+1} + r_j) \quad (28)$$

At the boundaries, $r_{1/2}=0$ and $r_{J+1/2}=R$.

The discrete ordinates method is a fairly direct, roughly finite difference, numerical solution to the radiative transfer equation. The method is not as intensive in computer time as one might suppose for this four dimensional problem, due to the reduction by quadrature to a fairly coarse directional mesh. The method is reasonably straightforward to program, although care must be taken to preserve its stability.

Prior applications of the discrete ordinates method in curvilinear coordinates have been expressed in the traditional directional coordinate system, based on a polar axis extended from the spatial radius vector. This study introduces the Spatially Axisymmetric Directional coordinate system, and also establishes the differencing method, eq.24, the directional coefficients, eq.25, and the quadrature, in the following section, for discrete ordinates method applications to spatially axisymmetric problems.

Quadrature

While the spatial mesh for numerical solution is chosen in a non-deterministic manner to suit the problem, the directional mesh is derived as a structured set of directions (ordinates) and their associated integration weights. The set of ordinates and weights is referred to collectively as a quadrature. Standard mathematical quadratures are available, such as Gauss, Chebyshev-Gauss, or Gauss-Legendre. However, these are generally spatially one-dimensional and Cartesian, and their use in the spherical directional distribution of radiation heat transfer calculations does not seem to impart any special accuracy (Abu-Shumays, 1977). More suitable quadratures have been proposed by Carlson and Lathrop (1968), and by Fiveland (1987) for spatially Cartesian geometries. Carlson and Lathrop's quadrature involves substitution of direction cosines for the directional angles in the radiative transfer equation, and construction of an ordered, symmetric set consistent for each Cartesian axis. A further condition is that the zeroth (area) and first (flux) moments of the direction cosines, summed with their weights over the unit directional sphere, equal the corresponding analytical integral over a symmetric octant of the directional unit sphere. Carlson and Lathrop's quadrature is not suitable for the present problem as the cosine formulation will not fit the axisymmetric boundary condition, and this quadrature has a tendency to favor the Cartesian coordinate directions; r and x in the plane of symmetry. Fiveland's

quadrature is suitable for one-dimensional problems, and extends the moment condition of Carlson and Lathrop to include the first n moments for an n -point quadrature. Fiveland noted that this quadrature produces very accurate results; however, the higher ranges of moments ($n \geq 2$) only have solutions which are consistent with the $n=0,1$ solutions if the moments are taken about the polar axis of the directional coordinate system. In the present case, this would result in a quadrature optimized for the direction normal to the plane of symmetry, which is not of particular concern here. For the present problem, the relevant moments are about an axis in the equatorial ($\alpha=\pi/2$) plane. Thus, an alternate quadrature to Carlson and Lathrop's or Fiveland's must be developed.

In the present two-dimensional case (as opposed to one-dimensional quadratures), each ordinate is specified by a pair (α_ℓ, γ_m) , where $1 \leq \ell \leq L$ and $1 \leq m \leq M$. Here the ℓ range represents a quarter circle (half of the half circle range of a polar angle), while the m range represents an entire circle, together covering a symmetric hemisphere. In specification of the associated weight, $w_{\ell m}$, the suggestion of Abu-Shumays (1977) is followed, letting $w_{\ell m} = w_\ell w_m$. Thus, the task of identifying a quadrature may potentially extend to $2(L+M)$ discrete values $(\alpha_\ell, w_\ell, \gamma_m, w_m)$. However, some simplifications may be made. Carlson (1971) and Fiveland (1987) noted that numerical stability of the radiation intensity computation was enhanced if all of the weights are equal, and the moment conditions are satisfied by the ordinates alone. Thus, $w_\ell = w_L$ is allowed for all ℓ , and likewise $w_m = w_M$ (therefore all $w_{\ell m} = w_\ell w_m$ are equal). It may be considered that the purpose of a quadrature is to

improve the accuracy of a particular quantity, at the expense of complete information on the distribution of other quantities. For instance, in a one-dimensional problem, the quadrature is chosen to enhance the accuracy of the radial direction heat flux calculation at the expense of information in non-radial directions. In the present problem, we are willing to sacrifice information on the distribution of intensity over α , which are rotations out of the plane of symmetry, except as the α ordinates impact on the computation of the distributions in the other coordinates. Thus, we chose a quadrature distribution for α . However, we do not wish to sacrifice the accuracy of distributions which lie in the plane of symmetry, and so we choose a problem-suited distribution of γ . Here, we choose an even distribution $\gamma_m = (m-1/2)\Delta\gamma$ and $w_m = \Delta\gamma$, where $\Delta\gamma = 2\pi/M$.

The remaining $L+1$ elements of our quadrature are w_L and α_ℓ , $1 \leq \ell \leq L$. Since Fiveland's higher moments are insoluble in this coordinate system, only the first two moments (zeroth and first) are specified, and an even cosine distribution for the remaining α_ℓ 's is chosen, thus favoring directions near $\alpha = \pi/2$. Thus $\alpha_\ell = (L+1/2 - \ell)[\Delta(\cos \alpha)]$, and:

$$\int_0^{\frac{\pi}{2}} \int_0^{\frac{\pi}{2}} \sin \alpha \, d\alpha \, d\gamma = \frac{\pi}{2} = \sum_{m=1}^{\frac{M}{4}} \sum_{\ell=1}^L w_\ell w_m \quad (29a)$$

$$\int_0^{\frac{\pi}{2}} \int_0^{\frac{\pi}{2}} \sin^2 \alpha \cos \gamma \, d\alpha \, d\gamma = \frac{\pi}{4} = \sum_{m=1}^{\frac{M}{4}} \sum_{\ell=1}^L \sin \alpha_\ell \cos \gamma_m w_\ell w_m \quad (29b)$$

serve to complete the quadrature. Equations 29 are solved to yield $w_\ell = 1/L$ and a value

for $\Delta(\cos \alpha)$. Although the n-moment accuracy of Fiveland's one-dimensional quadrature could not be recreated in this two-dimensional coordinate system, it should be noted that the derived quadrature has a similar philosophy to Carlson and Lathrop's quadrature for multi-dimensional spatially Cartesian problems, which is in standard use (Duderstadt and Martin, 1978, Lewis and Miller, 1984). In both quadratures, the zeroth (area) and first (flux) moments in the unit directional sphere are satisfied, and the remaining quadrature points are distributed to suit geometrical convenience.

Discretized Energy Equations

The continuous phase energy equation, eq.19a, is expressed in discretized form by multiplying by a differential element of volume, $2\pi r dr dx$, and rearranging:

$$\begin{aligned}
 & \pi (\rho c_p u)_c (r_{j+1/2}^2 - r_{j-1/2}^2) \left[T_{c,j,k+1/2} - T_{c,j,k-1/2} \right] \\
 & - 2\pi k (x_{k+1/2} - x_{k-1/2}) \left[r_{j+1/2} \frac{T_{c,j+1,k} - T_{c,j,k}}{r_{j+1} - r_j} - r_{j-1/2} \frac{T_{c,j,k} - T_{c,j-1,k}}{r_j - r_{j-1}} \right] \\
 & + T_{c,j,k} \left[4\sigma_b T_{c,j,k}^{*3} (4\kappa_c + 4\pi r_d^2 N q_{cd}') + 2\pi r_d N k \right] \pi (r_{j+1/2}^2 - r_{j-1/2}^2) (x_{k+1/2} - x_{k-1/2}) \\
 & = 3T_{c,j,k}^{*4} \sigma_b (4\kappa_c + 4\pi r_d^2 N q_{cd}') \pi (r_{j+1/2}^2 - r_{j-1/2}^2) (x_{k+1/2} - x_{k-1/2}) \\
 & + q_{cd}' 4\pi r_d^2 N \left[\sigma_b T_{d,j,k}^4 + \frac{k}{2r_d} T_{d,j,k} \right] \pi (r_{j+1/2}^2 - r_{j-1/2}^2) (x_{k+1/2} - x_{k-1/2}) \\
 & + \left[\kappa_c 2 \sum_{\ell=1}^L \sum_{m=1}^M I_{j,k,\ell,m} w_\ell w_m \right] \pi (r_{j+1/2}^2 - r_{j-1/2}^2) (x_{k+1/2} - x_{k-1/2}) \quad (30a)
 \end{aligned}$$

where the linearization $T^4 = 4TT^{*3} - 3T^{*4}$ has been used, and T^* is the best prior estimate of T . Note that the downstream conduction has been neglected as insignificant compared to the cross-stream conduction ($Pe = 2U_c R \rho_c c_{p,c} / k > 100$, Kays and Crawford, 1980). This improves the stability of a downstream marching algorithm. For a

cylindrical chamber with $Pe < 100$, the downstream conduction would have to be included.

The dispersed phase energy equation is left in derivative form, rather than cell difference form:

$$\begin{aligned}
 & (\rho c_p u)_d \frac{r_d}{3} \frac{T_{d,j,k+1/2} - T_{d,j,k-1/2}}{x_{k+1/2} - x_{k-1/2}} \\
 & + T_{d,j,k} \left[4T_{d,j,k}^3 (\epsilon_d \sigma_b + q_{cd}' \sigma_b) + \frac{k}{2r_d} \right] \\
 = & 3T_{d,j,k}^4 (\epsilon_d \sigma_b + q_{cd}' \sigma_b) + T_{c,j,k}^4 q_{cd}' \sigma_b + T_{c,j,k} \frac{k}{2r_d} \\
 & + \frac{\epsilon_d}{4} 2 \sum_{l=1}^L \sum_{m=1}^M I_{j,k,l,m} w_l w_m
 \end{aligned} \tag{30b}$$

In eqs.30, a linear cell form similar to eqs.26 is used to put the value at $x_{k+1/2}$ in terms of the values at x_k and $x_{k-1/2}$.

Computational Algorithm

The general algorithm for numerical solution is as follows: continuous and dispersed phase temperatures are estimated as the temperature at the last x (or the initial condition); the dispersed phase velocity is solved (the continuous phase velocity is set, as specified by eq.3b for a given U_c); (*) the radiative transfer equation is solved for the temperature estimates, producing the integrated intensity terms for the energy equations; the dispersed energy equation is solved using the most recent intensity solution and the continuous phase temperature estimate to yield the dispersed phase temperature; the continuous phase energy equation is solved using the most recent intensity and dispersed phase temperature solutions to yield the continuous phase temperature; the continuous and dispersed phase temperatures are compared to their

estimates; if the temperatures have all converged, the solution proceeds to the next x ; if the temperatures have not all converged, both temperature fields are over relaxed to form new estimates and iteration is continued from *. This process is illustrated in fig.7. The iterative solution accomplishes two purposes: convergence in the nonlinear energy equations; and convergence between the energy equations and the radiative transfer equation.

The dispersed phase velocity, for a given u_c , is the solution to eq.4c with the initial condition eq.5; however, this results in an implicit equation:

$$u_d = u_c + u_c (f_u^o - 1) \exp \left[f_u^o - \frac{\mu_c x}{32 \rho_d r_d^2} - u_d \right] \quad (31a)$$

Instead, the explicit equation for x is used:

$$x = \frac{32 \rho_d r_d^2}{\mu_c} \left\{ f_u^o u_c - u_d - u_c \ln \left(\frac{1 - u_d/u_c}{1 - f_u^o} \right) \right\} \quad (31b)$$

with a Newton searching algorithm. The algorithm starts from $u_d(r, x_{k-1})$, uses $\partial u_d / \partial x$ from eq.4c to make the initial guess of $u_d(r, x_k)$, uses eq.31b to test for convergence, and uses eq.31a to update the guess. The solution proceeds point by point across the stream. With the solution for u_d , N follows from eq.1c.

The radiative transfer solution (for given temperature) is also iterative. As an initial estimate, radiation intensity is set equal to blackbody intensity for a local mixture temperature, which is the absorption coefficient weighted average of the continuous and dispersed phase temperatures. This estimate is used to form the scattering term in the radiative transfer equation. The solution proceeds by spatial and directional marching procedures. (**) The spatial procedure is an outer loop, and starts at the first spatial point inside the tube wall, marching backwards, using eq.23c to provide the starting

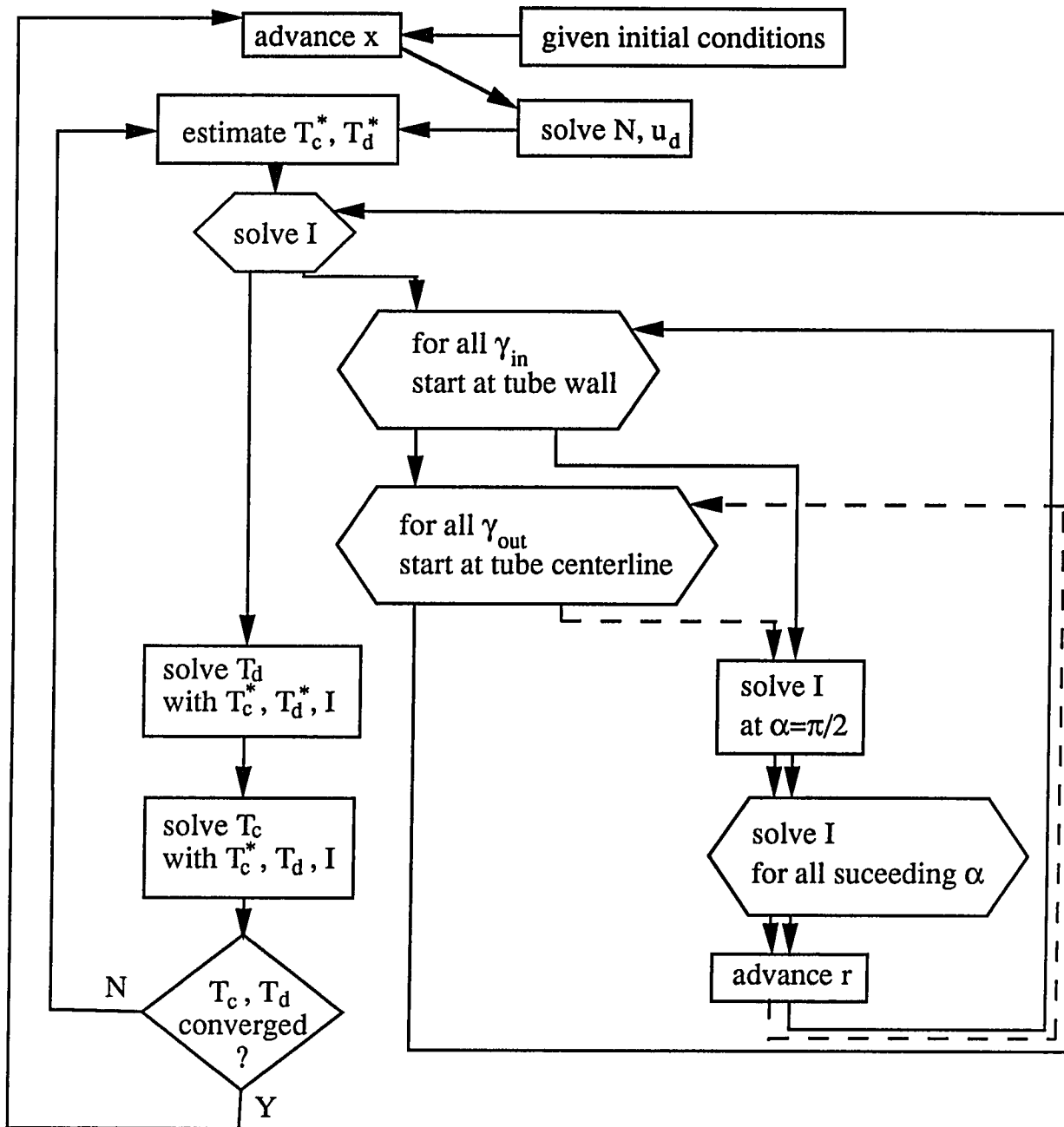


Figure 7 - Computational algorithm

$I_{j+1/2,k,\ell,m}$, and covering all inward facing γ . In applying eq.23c, the most recent intensity estimate is used to determine the reflection part. The directional marching procedure is an inner loop, and first solves the radiative transfer equation at $\alpha=\pi/2$, where $\partial I/\partial\alpha=0$. Using this solution to establish $I_{j,k,\ell+1/2,m}$, marching is completed over the range of ℓ . When the range of ℓ has been completed, the directional march (inner loop) at a spatial point is complete, and the algorithm proceeds to the next step of the spatial march (outer loop). This outer/inner routine proceeds to the centerline of the tube. At this point, the solution is complete for all r and α , inwards facing γ , and the current x . At the centerline, eq.23b (symmetry) is applied by making each $I_{1/2,k,\ell,m}$ for outward facing γ equal to the intensity for the complementary γ , which was solved on the inward spatial march. This ensures that there is no radiation heat flux across the centerline, and provides $I_{j-1/2,k,\ell,m}$ for the second spatial/directional marching procedure, which is for all outwards facing γ . From the centerline, the outer/inner routine continues, using backwards marching for ℓ as before, but now using forward marching for r . In this way, the solution of intensity for all r , α , and γ , and the current x , is completed. Now a convergence criterion is applied, but only to the integrated intensity term which appears in the energy equations. If not converged, a new scattering term is formed, and a new wall intensity is determined from eq.23c. The point ** is returned to, and the process continues until convergence is achieved. This process is also illustrated in fig.7.

In cases of low continuous phase absorption coefficient, the inner (α) marching

procedure can be unstable in backwards marching if the outer (r) procedure coefficients are increasing; i.e., for marching out from the center after having marched in. For decreasing spatial coefficients (decreasing radius) this does not occur. This effect is magnified at the very small radii near the tube centerline. This instability may be avoided by using the inward marching results to extrapolate an intensity for $\alpha=0$, which, being on the polar axis, is common for γ . The $\alpha=0$ direction corresponds to $\ell=1/2$, and this value may be used to start a stable forward α marching procedure for outward marching in r.

The radiative intensity solution requires known intensity at the last x, $I_{j,k-1/2,\ell m}$. However, there is no initial condition in x for intensity. The intensity solution is made by solving the intensity at $x=0$, where the temperatures are known (initial conditions). This initial intensity is solved by neglecting $\partial I/\partial x$ in favor of $\partial I/\partial r$ and $\partial I/\partial \alpha$. A last x intensity is then available for intensity solutions downstream. The discretization of $\partial I/\partial x$ can be destabilizing, and in some cases it is necessary to suppress $\partial I/\partial x$ (neglecting it in favor of $\partial I/\partial r$ and $\partial I/\partial \alpha$) for the first several steps downstream, before reintroducing it to the formulation.

Since there is no cross-stream dependence in the dispersed phase energy solution for T_d , other than indirectly through T_c , T_d may be solved explicitly from eq.30b within the main iteration loop. T_c is solved using an implicit formulation from eq.30a, which is tridiagonal, and may be solved with the efficient Thomas algorithm for tridiagonal matrix solution (Carnahan, et al, 1969). In both the continuous and dispersed energy formulations, it is important to include the temperature dependence of the redimensionalized interphase heat transfer terms on the left side of the equations;

instability results otherwise, indicating the important role played by interphase heat transfer. For the correct correlation of the coefficient q_{cd}' itself, it has been found to be sufficient to base q_{cd}' on the temperature estimate (T^*).

All discrete formulations in this study have been made to accommodate an irregular mesh. In r , it is important to have a fine mesh near the tube walls, as temperature varies rapidly here in combined mode heat transfer problems (Jones and Bayazitoglu, 1990). Variation with x is very rapid near the inlet, as the medium strives to meet the boundary conditions, but much less so further downstream. Generally, a logarithmic based x mesh is most useful (Bayazitoglu and Jones, 1990).

RESULTS AND DISCUSSION

Non-Dimensional Parameters

There are 18 dimensional parameters with an impact on the solution of the governing equations for continuous phase energy, dispersed phase momentum and energy, and radiation intensity. These are:

- Continuous phase properties

ρ_c gas density

c_{pc} gas specific heat

k gas thermal conductivity

μ_c gas viscosity

κ_c gas radiative absorption coefficient

u_c gas velocity

T_c gas temperature

- Dispersed phase properties

ρ_d particle material density

c_{pd} particle material specific heat

r_d particle radius

ϵ_d particle material surface emissivity

N particle number density

u_d particle velocity

T_d particle temperature

- Boundary properties

R tube radius

x axial length coordinate

T_w tube wall temperature

ϵ_w tube wall emissivity

Of the 18 dimensional parameters, four are variables (u_d , N , T_c , and T_d), while the rest are kept constant (or of constant distribution). By the Buckingham Π theory (Roberson and Crowe, 1975), given the four point basis of mass, length, time, and temperature, the 18 dimensional parameters may be reduced to 14 non-dimensional groups. The reference basis chosen for non-dimensionalization is: R , T_w , ρ_c , and U_c (as $u_c(r)/U_c$ is given, $u_c(r)$ may be represented by U_c). The dimensionless parameters chosen are relatively standard to combined mode heat transfer problems (Echigo, et al, 1972, Ozisik, 1973, Azad and Modest, 1981):

$Bo = \rho_c c_{p,c} U_c / \sigma_b T_w^3$ Boltzmann number

$Nr = (\kappa_c + \pi r_d^2 N) k / 4 \sigma_b T_w^3$ conduction to radiation ratio

$Pr = \mu_c c_{p,c} / k$ Prandtl number

$M_L = 4 \pi \rho_d r_d^3 N / 3 \rho_c$ mass loading ratio

$f_u = u_d / u_c$ phase velocity ratio

$f_p = \rho_d / \rho_c$ phase material density ratio

f_T	$=c_{pd}/c_{pc}$	phase specific heat ratio
r^*	$=R/r_d$	particle size parameter
τ_c	$=\kappa_c R$	continuous phase optical radius
ω_d	$=1-\varepsilon_d$	dispersed phase scattering albedo
ε_w	$=\varepsilon_w$	wall emissivity
θ_c	$=T_c/T_w$	dimensionless continuous phase temperature
θ_d	$=T_d/T_w$	dimensionless dispersed phase temperature
ξ	$=x/(R Bo)$	dimensionless axial length

Further, the mesh over R is represented by $\zeta=r/R$, the dimensionless continuous phase velocity is represented by $u_c^*=u_c/U_c$, and the shorthand $\tau_d=\pi r_d^2 N$ is used, where τ_d is the dispersed phase optical thickness.

Rewriting the governing equations in dimensionless form, the dispersed phase momentum equation is expressed:

$$u_c^* f_u \frac{\partial f_u}{\partial \xi} = \frac{Pr Nr \tau_d r^*}{24 M_L (\tau_c + \tau_d)} (1 - f_u) \quad (32)$$

The dispersed phase energy is expressed:

$$\begin{aligned} & \left[\frac{u_c^* f_u}{3 r^*} \frac{\partial \theta_d}{\partial \xi} + (1 - \omega_d) \left[\theta_d^4 - \int_0^\pi \int_0^{2\pi} I^* \sin \alpha \, d\gamma \, d\alpha \right] \right] \\ & = -q_{cd}' \left[(\theta_d^4 - \theta_c^4) + \frac{Nr r^*}{2(\tau_c + \tau_d)} (\theta_d - \theta_c) \right] \end{aligned} \quad (33)$$

where $I^* = I / \sigma_b T_w^4$ and the governing parameters for q_{cd}' are:

$$Pl = \frac{Nr r^*}{(\tau_d + \tau_c)} \quad (34a)$$

$$\kappa_c r_d = \frac{\tau_c}{r^*} \quad (34b)$$

$$\frac{T_d}{T_c} = \frac{\theta_d}{\theta_c} \quad (34c)$$

$$Pe = 2 u_c^* (f_u - 1) \frac{Bo (\tau_d + \tau_c)}{Nr r^*} \quad (34d)$$

Note in eq.34b the effect of tube to particle radius ratio, r^* . This parameter is unlikely to have a value much less than 100. The continuous phase optical thickness for most gases, for the tube diameters considered here, will be unlikely to exceed 10. Therefore,

the parameter $\kappa_c r_d$ will probably be less than 0.1 for particle-seeded furnace tubes, meaning, from fig.4, that eq.16 can be employed without loss of accuracy.

The continuous phase energy equation is expressed in dimensionless form:

$$\begin{aligned} \frac{u_c^*}{4} \frac{\partial \theta_c}{\partial \xi} - \frac{Nr}{(\tau_d + \tau_c)} \left[\frac{1}{\zeta} \frac{\partial}{\partial \zeta} \left(\zeta \frac{\partial \theta_c}{\partial \zeta} \right) + \frac{1}{Bo^2} \frac{\partial^2 \theta_c}{\partial \xi^2} \right] + \tau_c \left[\theta_c^4 - \int_0^{\pi} \int_0^{2\pi} I^* \sin \alpha \, d\gamma \, d\alpha \right] \\ = \tau_d q_{cd} \left[(\theta_d^4 - \theta_c^4) + \frac{Nr r^*}{2(\tau_c + \tau_d)} (\theta_d - \theta_c) \right] \end{aligned} \quad (35)$$

The radiative transfer equation is expressed in dimensionless form:

$$\begin{aligned} \frac{1}{\zeta} \sin \alpha \cos \gamma \frac{\partial}{\partial \zeta} (I^* \zeta) - \frac{1}{Bo} \sin \alpha \sin \gamma \frac{\partial I^*}{\partial \xi} + \frac{1}{\zeta} \cos \gamma \frac{\partial}{\partial \alpha} (I^* \cos \alpha) + (\tau_d + \tau_c) I^* \\ = \frac{\tau_c}{\pi} \theta_c^4 + (1 - \omega_d) \frac{\tau_d}{\pi} \theta_d^4 + \frac{\omega_d \tau_d}{4\pi} \int_0^{\pi} \int_0^{2\pi} p(\alpha, \gamma, \tilde{\alpha}, \tilde{\gamma}) I^*(\tilde{\alpha}, \tilde{\gamma}) \sin \tilde{\alpha} \, d\tilde{\gamma} \, d\tilde{\alpha} \end{aligned} \quad (36)$$

Verification

In order to verify the numerical algorithm, tests were run against the results of Heaslet and Warming (1966, as presented in Azad and Modest, 1981b) for radiation heat flux in scattering media with prescribed temperature profile, and also against the results of Echigo, et al, 1972 for a laminar gas/particle flow with non-scattering particles, a non-radiatively participating gas, and no initial interphase temperature difference. Both of these analyses are for non-axially varying intensity. In addition to verifying the solution for these cases, this procedure allowed the development of suitable mesh sizes and distributions. The previous results were met using a quadrature of four points in the half range of α (a $\Delta(\cos \alpha)$ of 0.2545 meets the moment criteria) and 16 points in the full range of γ . An irregular radial mesh of 25 points was used, with $\Delta\zeta$ varying from 0.05 at the tube centerline to 0.01 at the tube wall. A logarithmic mesh of 30 points was used in ξ , covering four decades up to $\xi=1$. This mesh gave

results within 1% of all the studied results of the previous investigations. For a given x , five to ten iteration cycles are generally necessary to converge the energy equations to within 0.1%. Convergence of the radiative transfer equation depends on ω_d and ϵ_w . For $\epsilon_w=1$ and $\omega_d=0$, the intensity is solved directly. For $\omega_d=0.5$, on the order of ten iterations are required. For $\epsilon_w=1$, $\omega_d=0$, and the mesh given above, run times have been approximately 30 minutes on an 8 megabit super-minicomputer.

Behavior of a Base Case

In figs.8a, b, and c, temperature profiles for both phases are shown at $\xi=0.001$, 0.01, and 0.1, respectively, for a base case where $\theta_{c,o}=0.5$, $\theta_{d,o}=0.8$ (initial temperatures), $\tau_c=1$, $Nr=1$, $r^*=100$, $M_L=1$, $f_p=1000$, $f_{u,o}=1$, $Pr=1$, $f_T=1$, $\epsilon_w=1$ (black walls), $\omega_d=0$, and $Bo=100$. In fig.8a, the initial temperature profiles are beginning to alter to meet the boundary condition $\theta_w=1$. Note that there is no cross-stream boundary condition for θ_d , as a temperature jump is allowed between the dispersed phase and the wall. θ_c alters to meet the temperature boundary condition, while θ_d is affected by the wall intensity boundary condition. The slight dip in θ_d at the edge of the developing boundary layer is due to the higher relative effect of the interphase heat transfer terms in the dispersed phase energy equation where the velocity, and hence convective heat transfer, is low. In fig.8b, further downstream, the core temperatures continue to

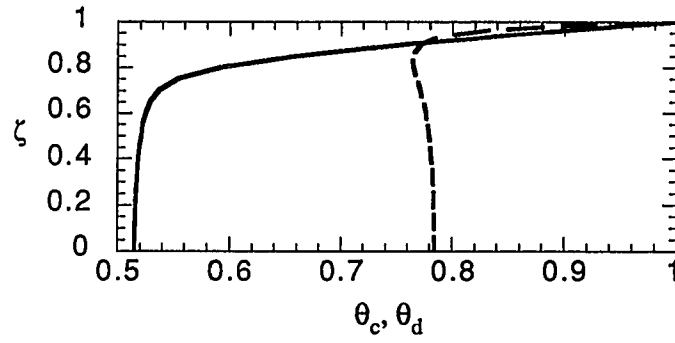
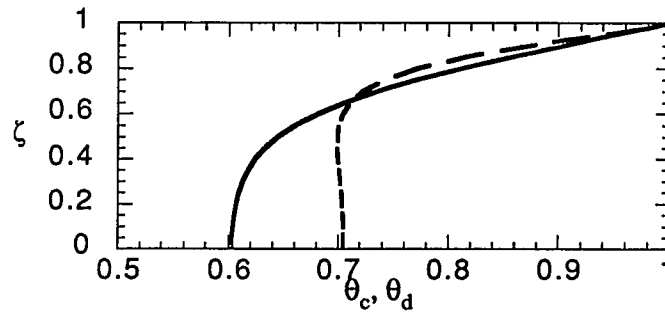
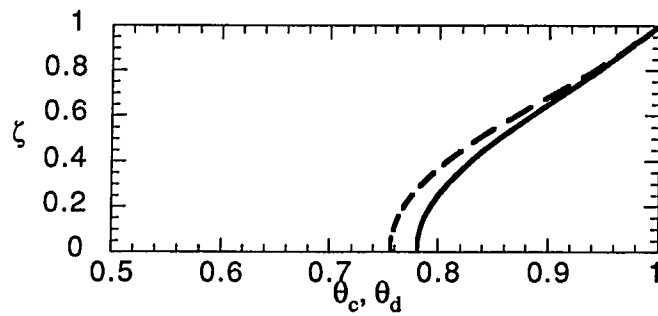
fig.8a - $\xi=0.001$ fig.8b - $\xi=0.01$ fig.8c - $\xi=0.1$

Figure 8 - Temperature profiles at different cross-sections downstream for a gas/particle flow with the base case parameters.

approach each other, responding to interphase heat transfer, while boundary layers along the wall continue to develop. The dispersed phase temperatures lag behind the continuous phase temperatures in the boundary layer because of the value of the conduction to radiation ratio, $Nr=1$. Nr is a ratio of conduction like terms to radiation like terms, and does not necessarily correlate the magnitude of the respective modes of heat transfer. Generally, $Nr=1$ is high enough to favor conduction over radiation (Ozisik, 1973). In fig.8c, the boundary layers are fully developed. The dispersed phase temperature in the core, which started off hot, has been cooled by the continuous phase and is now lagging behind the continuous phase due to relatively lower radiative transfer from the walls, but not divergently lower, due to interphase heat transfer. Similar effects were demonstrated by Echigo, et al, (1972).

The remaining results are given in terms of the tube's function as a heat exchange tube in a furnace (the combustion bed). Heat exchange parameters are defined by the continuous phase, as it is the gas which is to benefit from introduction of the particles.

Heat exchange effectiveness is defined at a given cross-section (given value of ξ) by the wall temperature (assumed to remain constant) and the mean continuous phase temperature across the cross-section:

$$\epsilon_{eff} = \frac{2 \int_0^1 \zeta \theta_c d\zeta - \theta_{c,o}}{1 - \theta_{c,o}} \quad (37)$$

where $\theta_{c,o}$ is the initial dimensionless temperature. The number of transfer units to the continuous phase, Ntu , is defined in dimensional terms by:

$$Ntu(x) = \frac{1}{\dot{m}_c c_{pc}} \int_0^x \left[\frac{Q_{wall}' + Q_{particles}'}{T_w - T_{c,m}} \right] dx \quad (38a)$$

where Q_{wall}' and $Q_{particles}'$ are the heat input to the continuous phase per unit length from, respectively, the wall and the particles, $T_{c,m}$ is the cross-sectional mean continuous phase temperature, and the expression is non-dimensionalized by the heat capacity rate. Equation 38a may be written in dimensionless form:

$$Ntu(\xi) = 2 \int_0^\xi \frac{\frac{4Nr}{\tau_c} \frac{\partial \theta_c(\zeta=1)}{\partial \zeta} - Q_w^* + Q_{cd}^*}{1 - 2 \int_0^1 \zeta \theta_c d\zeta} d\xi \quad (38b)$$

where:

$$Q_w^* = \frac{\tau_c}{\tau_c + \tau_d} \int_0^\pi \int_0^{2\pi} I^*(\zeta=1) \sin^2 \alpha \cos \gamma d\gamma d\alpha \quad (38c)$$

$$Q_{cd}^* = 4 \int_0^1 q_{cd}' \tau_d \left[(\theta_d^4 - \theta_c^4) + \frac{Nr r^*}{2 \tau_c} (\theta_d - \theta_c) \right] \zeta d\zeta \quad (38d)$$

The fraction of Ntu which comes from the particles, as opposed to the wall, is of interest. This fraction may be determined from the ratio of eq.38d to the numerator of eq.38b, integrated over ξ . Also of interest is the heat flux at the tube wall,

$q_w^* = q_w / \sigma_b T_w^4$, which is being carried away by the combined gas/particle mixture, and

which is necessary to maintain the boundary condition T_w :

$$q_w^* = \frac{4Nr}{\tau_c} \frac{\partial \theta_c(\zeta=1)}{\partial \zeta} - \int_0^\pi \int_0^{2\pi} I^*(\zeta=1) \sin^2 \alpha \cos \gamma d\gamma d\alpha \quad (39)$$

Figures 9a, b, and c show the downstream heat transfer properties associated with figs.8. Figure 9a shows the number of transfer units, Ntu , to the continuous phase as a function of ξ . Ntu increases steadily up to a ξ of about 0.01, and then increases at a lower rate. Figure 9b shows the fraction of Ntu which is due to the particles, as opposed to heat transfer to the continuous phase from the walls. Correlating with figs.8, the particle contribution is between 30% and 50% while there is a large temperature difference between the phases. As the continuous phase temperature comes up to the particle temperature and exceeds it, this fraction reduces and eventually becomes negative as the cooled particles remove heat from the continuous phase. The base parameters considered here do not lead to a case where additional heat flows from the walls to the particles by radiation, and thence to the gas. Here, heating of the gas by the particles is due to the initial temperature difference, and the advantage of injecting heated particles is spent once the tube length exceeds $\xi=0.01$. Figure 9c shows the wall heat flux necessary to keep up the temperature boundary condition. This is very high at the outset, due to the initial temperature differences with the wall, and declines as the gas/particle mixture is heated.

Variation of Individual Parameters

Starting from the same base set of parameters as figs.8 and 9, fig.10 shows the effect on heat exchange effectivity of varying the mass loading ratio of particle mass to gas mass. Low M_L , ≤ 0.1 , has little effect on the heat exchange tube's effectivity. For $M_L=1$, for low ξ , effectivity is improved. For ξ beyond the point at which the particles are no longer heating the gas, effectivity is impaired. As M_L is increased, this effect of initial improvement followed by impairment is emphasized. Qualitatively, this might be

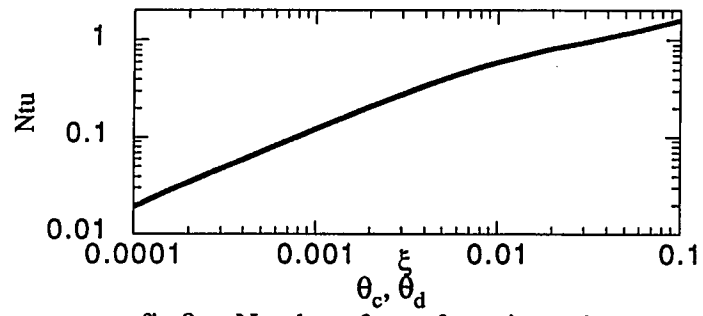


fig.9a - Number of transfer units to the gas

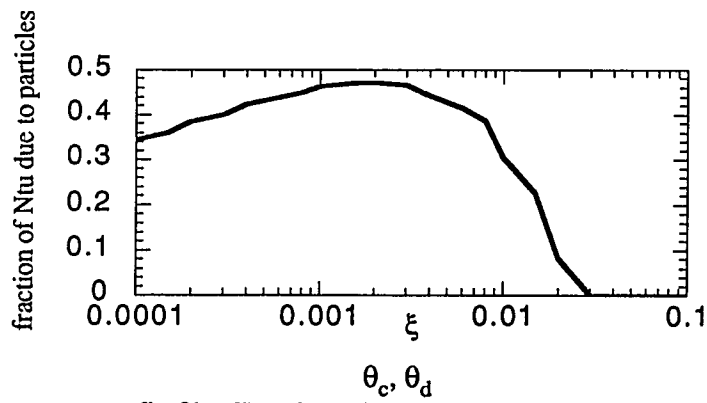


fig.9b - Fraction of Ntu due to the particles

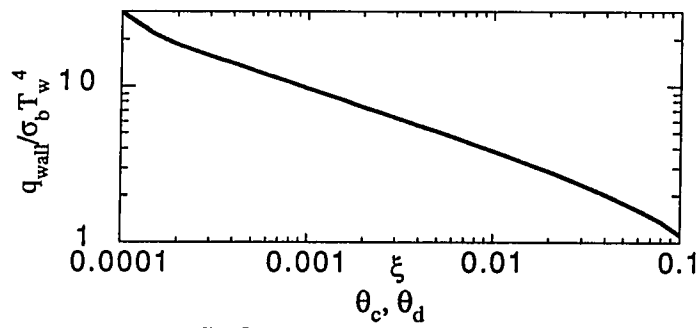


fig.9c - Heat flux at the tube wall

Figure 9 - Heat flux parameters as functions of downstream distance for a gas/particle flow with the base case parameters.

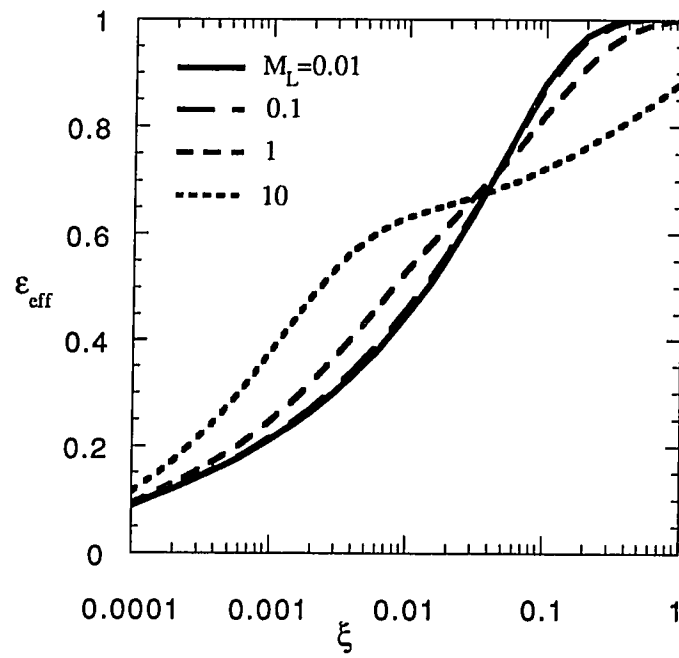


Figure 10 - Heat exchange effectivity for the gas: all base case parameters constant except for mass loading ratio, M_L .

expected as a result of the effect of seeding the gas with more and more hot material.

Figure 11 shows the effect of increasing the tube to particle radius ratio, r^* . As r^* is increased, the optical thickness of the dispersed phase increases as a result of the greater total surface area of the dispersed phase at constant M_L . Also, for constant Nr , increasing τ_d decreases k . These effects combine to make dispersed phase radiation the dominant mode of heat transfer in the gas/particle medium. However, for high optical thickness, heat flux at the edges of a medium is low (Bayazitoglu and Jones, 1990). Thus, for high r^* , the phase temperatures quickly come to equilibrium as a result of the large interphase area, but gain heat from the walls at a slow rate, due to the insulating effect of high optical thickness. This behavior is illustrated in fig.11, where as r^* is increased, effectivity is enhanced for short ξ , but impaired for longer tubes.

Figure 12 illustrates the effect of increased optical thickness directly, by varying the optical thickness of the continuous medium, τ_c . Again, it must be noted that for constant Nr , as τ_c is increased, k is reduced. As a result, optical insulation and reduced conduction are imposed on the medium simultaneously, with a predictable effect on heat exchange effectivity.

Figure 13 demonstrates the effect of varying the conduction to radiation ratio, Nr , with all other parameters held constant. Since optical thickness is constant, varying Nr in effect translates directly to variation of k .

Figure 14 shows the effect of varying the particle inlet temperature; in effect, it shows the value of reheating the particles and reinjecting them into the heat exchange tube. With reference to fig.10, the phenomenon demonstrated here is to delay the transition point at which the gas passes from being heated by the particles to where the

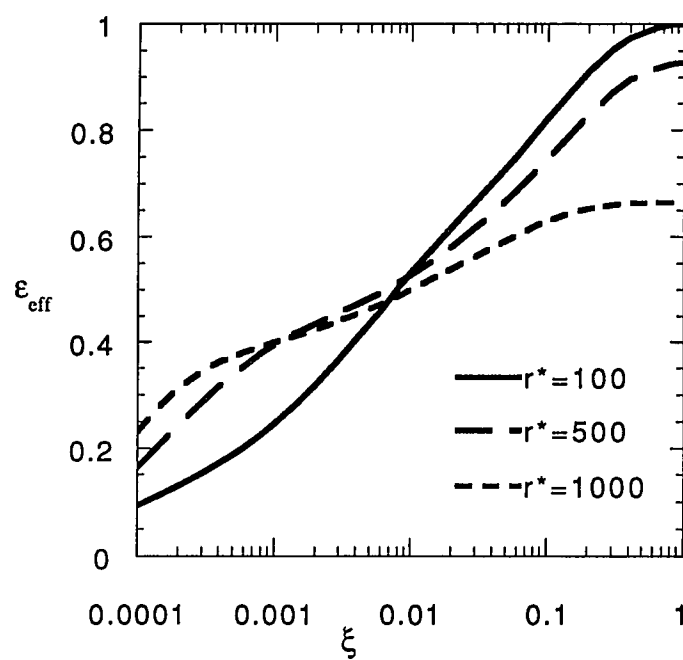


Figure 11 - Heat exchange effectivity for the gas: all base case parameters constant except for tube to particle radius ratio, r^* .

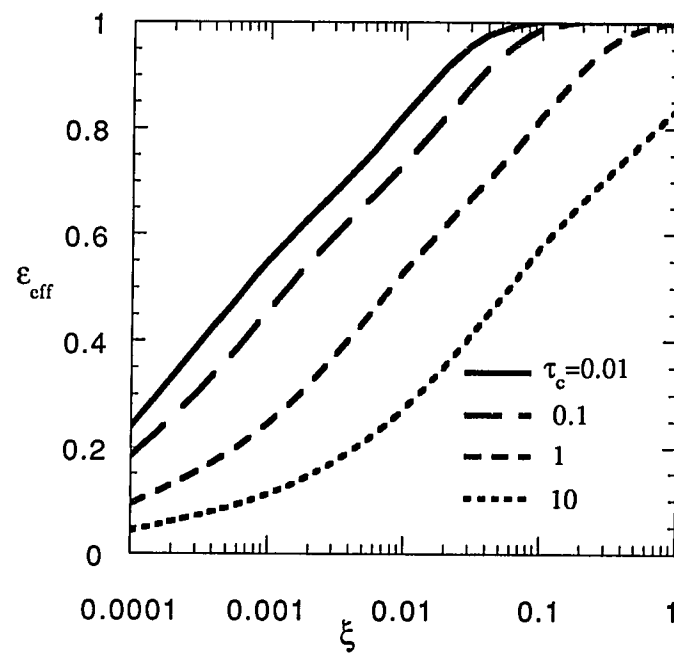


Figure 12 - Heat exchange effectivity for the gas: all base case parameters constant except for gas optical thickness, τ_c .

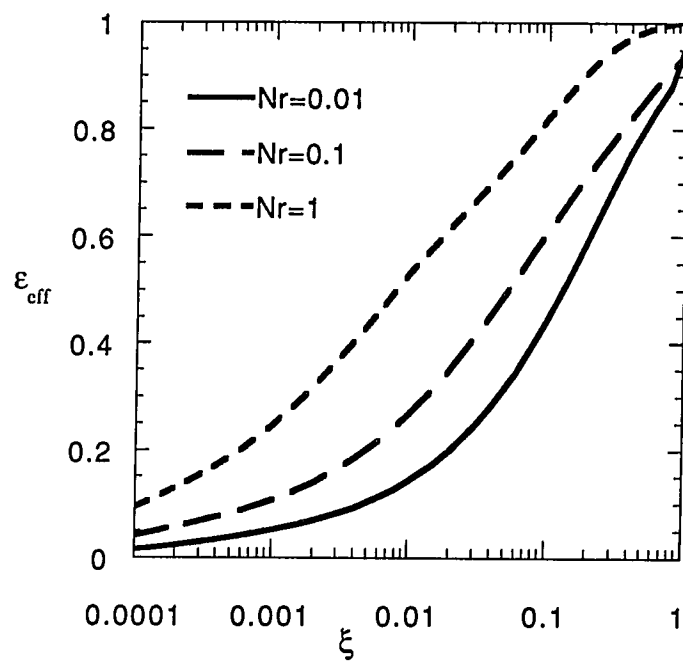


Figure 13 - Heat exchange effectivity for the gas: all base case parameters constant except for conduction to radiation ratio, Nr .

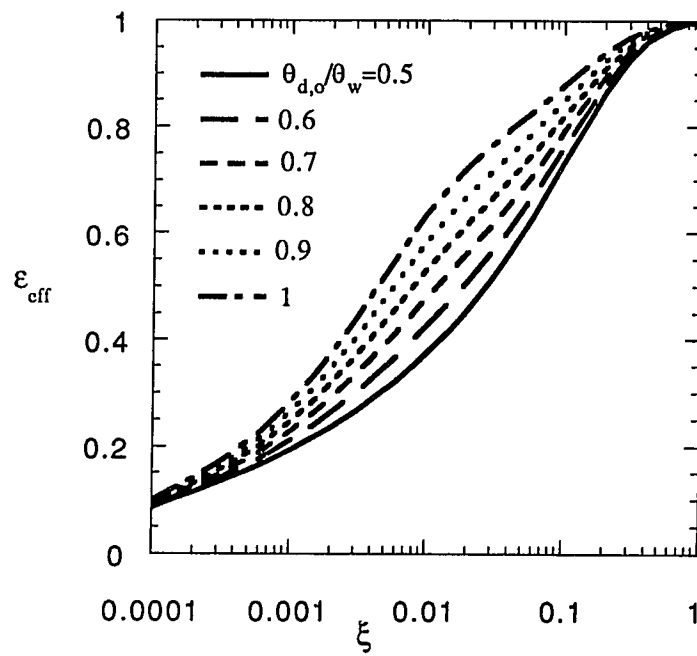


Figure 14 - Heat exchange effectivity for the gas: all base case parameters constant except for particle injection temperature, $\theta_{d,o}$.

particles are being heated by the gas. For extremely short tubes, $\xi < 0.0001$, injection temperature has little effect, as the rate of interphase heat transfer lags briefly behind the immediate effect of the wall temperature conductive boundary condition. For very long tubes, $\xi > 1$ (for the base set of other parameters), it can be seen that the gas will be heated to the wall temperature eventually regardless of particle temperature. For intermediate ξ , the impact of increased particle inlet temperature on heat exchange effectivity can be significant.

Most other parameters have only a minor effect on the heat exchange effectivity, or mirror the effects of other parameters. The material density ratio f_p , for constant mass loading ratio, in effect varies the optical thickness downwards with the same effect as for other parameters which accomplish this. The initial velocity ratio between particles and gas had very little effect on heat transfer. Higher particle velocities persisted well into the tube, but considering the inverse effect of r^* on the interphase Peclet number, eq.34d, there is little increased interphase heat transfer, and the convective effect on the overall flow of u_d at, say, twice u_c , is found to be minor. The specific heat ratio, f_T , was not varied, nor was the wall emissivity, ϵ_w , or the gas inlet temperature. The dispersed phase scattering albedo was varied over the range $0 \leq \omega_d \leq 1$. High scattering was found to reduce heat exchange effectivity by about 10% for the base parameters tested, fairly uniformly over ξ . The effect of Prandtl number, Pr , is only reflected in the drag on the particles at unequal interphase velocity. Since the effect of velocity ratio is small, Pr was not varied. The effect of Boltzmann number, Bo , is mostly reflected in the non-dimensionalization $\xi = x/(R Bo)$. Direct effects of Bo

for constant ξ are small.

Example Calculation

As a means of demonstrating the enhancement of heat transfer in a tube as a result of particle seeding, the following situation is considered: Steam at 500 K and about 10 atmospheres pressure enters a 2 cm diameter tube with a mean velocity of 1 m/s, which passes through a fluidized coal combustion bed at 1000 K. It is desired that the steam be heated to 800 K (effectivity $\epsilon_{\text{eff}}=0.6$). Constant properties are assumed, with: $\rho_c=3 \text{ kg/m}^3$, $c_{pc}=2000 \text{ J/kgK}$, $k=0.06 \text{ W/mK}$, $\mu_c=0.00003 \text{ kg/ms}$, and $\kappa_c=70 \text{ /m}$ (Ozisik, 1973, using a Planck mean coefficient). It is assumed that the seeding particles are some ceramic or stone like material, with $r_d=100 \text{ }\mu\text{m}$, $\rho_d=2500 \text{ kg/m}^3$, $c_{pd}=800 \text{ J/kgK}$, and $\epsilon_d=1$, injected into the tube at the gas speed and at 800 K. The dimensionless parameters for this example are: $\theta_{c,o}=0.5$, $\theta_{d,o}=0.8$, $\tau_c=0.7$, $r^*=100$, $f_p=833$, $f_{u,o}=1$, $Pr=1$, $f_T=0.4$, $\epsilon_w=1$ (black walls), $\omega_d=0$ (black particles), and $Bo=106$. The mass loading ratio and conduction to radiation ratio are related to N , the particle number density, by $M_L=3.49 \times 10^{-9} \text{ m}^3 N$ and $Nr=0.0185+8.31 \times 10^{-12} \text{ m}^3 N$ (or $Nr=0.0185+0.00238 M_L$).

Figure 15 shows the effectivity for the example case at $M_L=0$, 1, and 10. $M_L=0$ corresponds to a radiatively participating gas with no particles. For $M_L=0$, the heat exchange tube must be $\xi=0.212$ in length ($x=225 \text{ mm}$) to achieve the effectivity

requirement. For $M_L=1$, $\xi=0.189$ is sufficient ($x=200$ mm), an 11% reduction. For $M_L=10$, $\xi=0.089$ ($x=94$ mm) will allow $\epsilon_{\text{eff}}=0.6$, a 58% reduction in tube length. At $M_L=10$, the volume fraction of the particles is 1.2% and the average interparticle separation is 8.73 times the particle radius.

Figure 16 shows effectivity for the example case at $M_L=1$ and 10, with $\tau_c=0$ and 0.7. The $\tau_c=0$ result corresponds to a model similar to Echigo, et al (1972) or Azad and Modest (1981b), where radiative participation by the gas is not considered. At $M_L=1$, a considerable part of the overall absorption coefficient is due to the continuous phase, and neglecting it can lead to significant errors. For $M_L=10$, the absorption coefficient of the particles is high enough to essentially mask neglect of the gas absorption.

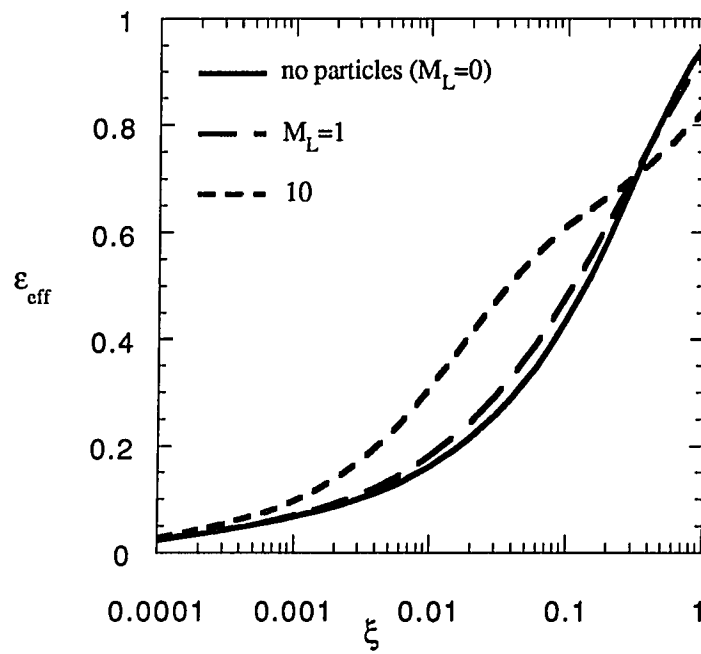


Figure 15 - Heat exchange effectiveness for the gas: example case with no seeding particles, with $M_L=1$, and with $M_L=10$.

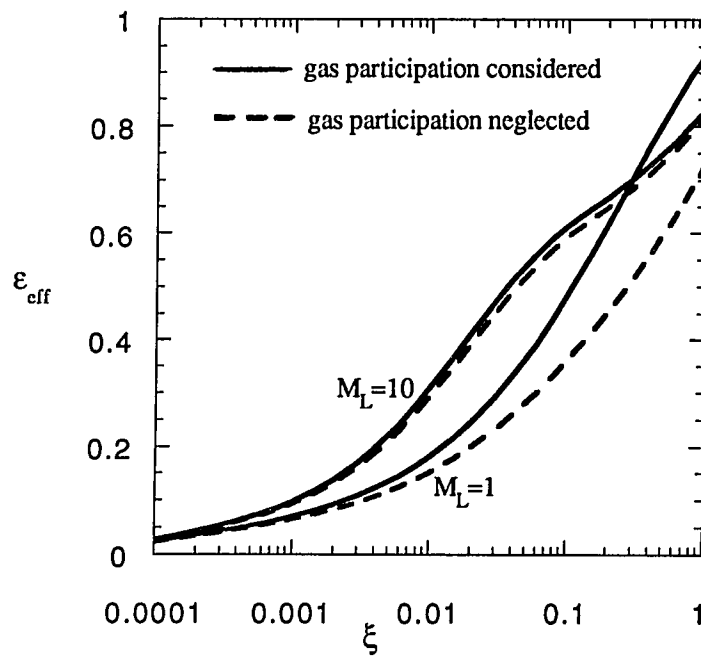


Figure 16 - Heat exchange effectivity for the gas: example case comparison between present model and model neglecting radiative participation of the gas.

CONCLUSIONS

In this study, a model is developed for combined radiation, conduction and convection heat transfer in dispersed two phase flow of gray, laminar, axisymmetric media with significant interphase temperature differences. The model extends treatment of such flows by considering radiative participation of the continuous phase using an accurate numerical model for solution of the radiative transfer equation. The model is formed of discrete parts expressing radiation intensity, energy conservation in each phase, and dispersed phase momentum. As such, the model may readily be extended to treat non-gray and turbulent cases.

In order to treat fully spatially axisymmetric problems, in which the frequent assumption of azimuthal symmetry for the radiation intensity directional dependence does not hold, a new coordinate system is developed. The Spatially Axisymmetric Directional coordinate system allows unrestrained variation of intensity parallel to the plane of symmetry, and provides a correct boundary condition for directional rotations out of the plane of symmetry. Expressions for the path derivative of radiation intensity in the new coordinate system are provided for spatially cylindrical and spatially spherical coordinates.

The discrete ordinates method is used for solution of the radiative transfer equation. This method is highly adaptable to combined mode heat transfer calculations due to its differential nature, straightforward concepts, and adaptability to variable properties, scattering functions, and boundary conditions. The discrete ordinates method has been extended to the Spatially Axisymmetric Directional coordinate system by deriving balanced discretized expressions of the radiative transfer equation in spherical and cylindrical coordinate systems; also, a quadrature of comparable accuracy to other widely used quadratures has been developed for the new coordinate system.

It is proposed that heat transfer in furnace tubes could be enhanced by injection of

heated particles into the gas stream. This method is shown to significantly reduce the necessary tube length in cases of high particle mass loading and high initial interphase temperature difference. The later indicates the value of reheating and recycling the seeding particles in a closed cycle. Mass loading ratios for the flow of seeding particle mass to carrying fluid mass must generally be greater than one, and as high as ten, for heat exchange enhancement to be significant. Decreasing the size of the seeding particles relative to the tube radius is also advantageous, especially for short tubes.

In order to verify interphase heat transfer correlations for combined radiation, conduction, and convection acting between the dispersed and continuous phases, combined mode heat transfer is formally modeled for a sphere in motion in an infinite fluid. It is found that in radiation dominant cases, the required practical extent of the "infinite" medium is considerably less than in conduction dominated cases. In cases with small particles and a low continuous medium absorption coefficient, so that the product $\kappa_c r_d$ is less than 0.1, a simplified correlation for combined mode heat transfer is found to be accurate. For higher $\kappa_c r_d$, heat transfer is overestimated by the simple correlation. However, the case of heated particle seeding of gas filled furnace tubes corresponds to relatively low $\kappa_c r_d$.

REFERENCES

- Anderson, D.A., Tannehill, J.C., and Pletcher, R.H., (1984), *Computational Fluid Mechanics and Heat Transfer*, Hemisphere Publishing Corporation, Washington, D.C.
- Abu-Shumays, I.K., (1977), "Compatible Product Angular Quadrature for Neutron Transport in x-y Geometry", *Nuclear Science and Engineering*, v.64, pp.299-316.
- Azad, F.H., and Modest, M.F., (1981a), "Combined Radiation and Convection in Absorbing, Emitting, and Anisotropically Scattering Gas-Particulate Tube Flow", *International Journal of Heat and Mass Transfer*, v.24, n.10, pp.1681-1698.
- Azad, F.H., and Modest, M.F., (1981b), "Evaluation of the Radiative Heat Flux in Absorbing, Emitting, and Linear-Anisotropically Scattering Cylindrical Media", *Journal of Heat Transfer*, v.103, n.2, pp.350-356.
- Bayazitoglu, Y., and Higenyi, J., (1979), "Higher-Order Differential Equations of Radiative Transfer: P_3 Approximation", *AIAA Journal*, v.17, n.4, pp.424-431.
- Bayazitoglu, Y., and Jones, P.D., (1990), "Enclosure and Conductive Effects on Thermal Performance of Liquid Droplet Radiators", *Journal of Thermophysics and Heat Transfer*, v.4, n.2, pp.186-192, April.
- Bayazitoglu, Y., and Ozisik, M.N., (1988), *Elements of Heat Transfer*, McGraw-Hill, New York.
- Bayazitoglu, Y., and Suryanarayana, P.V.R., (1989), "Transient Radiative Heat Transfer From a Sphere Surrounded by a Participating Medium", *Journal of Heat Transfer*, v.111, n.3, pp.713-718, August.
- Boure, J.A., and Delhay, J.M., (1982), "General Equations and Two Phase Flow Modeling", *Handbook of Multiphase Systems*, G. Hetsroni (ed.), Hemisphere Publishing Corporation, Washington, D.C.
- Brewster, M.Q., and Tien, C.L., (1982a), "Radiative Transfer in Packed Fluidized Beds: Dependent versus Independent Scattering", *Journal of Heat Transfer*, v.104, n.4, pp.573-579.
- Brewster, M.Q. and Tien, C.L., (1982b), "Examination of the Two Flux Model for Radiative Transfer in Particular Systems", *International Journal of Heat and Mass Transfer*, v.25, n.12, pp.1905-1907.
- Buckius, R.O., and Hwang, D.C., (1980), "Radiation Properties for Polydispersions: Application to Coal", *Journal of Heat Transfer*, v.102, pp.99-103.
- Carlson, B.G., (1971), *Tables of Equal Weight Quadrature EQ_n Over the Unit Sphere*, Los Alamos Scientific Laboratory report no. LA-4734, July.
- Carlson, B.G., (1970), *Transport Theory: Discrete Ordinate Quadrature over the Unit Sphere*, Los Alamos Scientific Laboratory report no. LA-4554, September.

Carlson, B.G., and Lathrop, K.D., (1968), "Transport Theory: the Method of Discrete Ordinates", in Greenspan, H., Kelber, C.N., and Okrent, D. (eds.), *Computing Methods in Reactor Physics*, Gordon and Breach, New York.

Carnahan, B., Luther, H.A., and Wilkes, J.O., (1969), *Applied Numerical Methods*, John Wiley and Sons, New York.

Chandrasekhar, S., (1950), *Radiative Transfer*, Clarendon Press, Oxford.

Chawla, T.C., and Chan, S.H., (1980), "Combined Radiation Convection in Thermally Developing Poiseuille Flow with Scattering", *Journal of Heat Transfer*, v.102, n.2, pp.297-302.

Clift, R., Grace, J.R., and Weber, M.E., (1978), *Bubbles, Drops, and Particles*, Academic Press, New York.

Crowder, R.S., Daily, J.W., and Humphrey, J.A.C., (1984), "Numerical Calculation of Particle Dispersion in a Turbulent Mixing Layer Flow", *Journal of Pipelines*, v.4, pp.159-169.

Crowe, C.T., (1979), *"Gas/Particle Flow"*, Pulverized Coal Combustion and Gasification, L.D. Smoot and D.T. Pratt (eds.), Plenum Press, New York.

Desoto, S., (1968), "Coupled Radiation, Conduction, and Convection in Entrance Flow", *International Journal of Heat and Mass Transfer*, v.11, pp.39-53.

Drolen, B.L., and Tien, C.L., (1987), "Independent and Dependent Scattering in Packed-Sphere Systems", *Journal of Thermophysics and Heat Transfer*, v.1, pp.63-68.

Duderstadt, J.J. and Martin, W.R., (1979), *Transport Theory*, John Wiley and Sons, New York.

Echigo, R., and Hasegawa, S., (1972a), "Radiative Heat Transfer by Flowing Multiphase Medium - Part I. An Analysis on Heat Transfer of Laminar Flow Between Parallel Flat Plates", *International Journal of Heat and Mass Transfer*, v.15, pp.2519-2534.

Echigo, R., Hasegawa, S., and Tamehiro, H., (1972b), "Radiative Heat Transfer by Flowing Multiphase Medium - Part II. An Analysis on Heat Transfer of Laminar Flow in an Entrance Region of Circular Tube", *International Journal of Heat and Mass Transfer*, v.15, pp.2595-2610.

Faeth, G.M., (1983), "Evaporation and Combustion of Sprays", *Progress in Energy and Combustion Science*, v.9, pp.1-76.

Fiveland, W.A., (1984), "Discrete-Ordinates Solutions of the Radiative Transport Equation for Rectangular Enclosures", *Journal of Heat Transfer*, v.106, pp.699-706.

Fiveland, W.A., (1987), "Discrete Ordinate Methods for Radiative Heat Transfer in Isotropically and Anisotropically Scattering Media", *Journal of Heat Transfer*, v.109, pp.809-812.

- Fiveland, W.A., (1988), "Three-Dimensional Radiative Heat-Transfer Solutions by the Discrete-Ordinates Method", *Journal of Thermophysics and Heat Transfer*, v.2, pp.309-316.
- Flamant, G., and Menigault, T., (1987), "Combined Wall to Fluidized Bed Heat Transfer; Bubbles and Emulsion Contributions at High Temperature", *International Journal of Heat and Mass Transfer*, v.30, n.9, pp.1803-1812.
- Gat, N., (1987), "The Circulating Balls Heat Exchanger", *Journal of Thermophysics and Heat Transfer*, v.1, n.2, pp.105-111, April.
- Glicksman, L.R., and Decker, N., (1982), "Heat Transfer from an Immersed Surface to Adjacent Particles in a Fluidized Bed: the Role of Radiation and Particle Packing", *Heat Transfer 1982, Proceedings of the Seventh International Heat Transfer Conference*, v.6, pp.45-50, Hemisphere Publishing Corporation, Washington, D.C.
- Glicksman, L.R., Azzola, J., and Modlin, J., (1988), "Fluidized Bed Solar Collector", *Journal of Solar Energy Engineering*, v.110, n.4, pp.321-326.
- Goodwin, D.G., and Ebert, J.L., (1987), "Rigorous Bounds on the Radiative Interaction Between Real Gases and Scattering Particles", *Journal of Quantitative Spectroscopy and Radiative Transfer*, v.37, n.5, pp.501-508.
- Goshayeshi, A., Welty, J.R., Adams, R.L., and Alavizadeh, N., (1986), "Local Heat Transfer Coefficients for Horizontal Tube Arrays in High-Temperature Large-Particle Fluidized Beds: an Experimental Study", *Journal of Heat Transfer*, v.108, n.4, pp.907-912.
- Harris, J.A., (1989), "Solution of the Conduction/Radiation Problem with Linear-Anisotropic Scattering in an Annular Medium by the Spherical Harmonics Method", *Journal of Heat Transfer*, v.111, n.1, pp.194-197.
- Heaslet, M.A., and Warming, R.F., (1966), "Theoretical Predictions of Radiative Transfer in a Homogeneous Cylindrical Medium", *Journal of Quantitative Spectroscopy and Radiative Transfer*, v.6, n.6, pp.751-774.
- Howell, J.R., (1988), "Thermal Radiation in Participating Media: the Past, the Present, and Some Possible Futures", *Journal of Heat Transfer*, v.110, n.4(B), pp.1220-1229.
- Hruby, J., Steeper, R., Evans, G., and Crowe, C., (1988), "An Experimental and Numerical Study of Flow and Convective Heat Transfer in a Freely Falling Curtain of Particles", *Journal of Fluids Engineering*, v.110, n.2, pp.172-181.
- Jones, P.D., and Bayazitoglu, Y., (1990), "Combined Radiation and Conduction from a Sphere in a Participating Medium", presented at the 9th International Heat Transfer Conference, Jerusalem, Israel, 19-24 August.
- Kays, W.M. and Crawford, M.E., (1980), *Convective Heat and Mass Transfer*, 2nd ed., McGraw-Hill, New York.

Kumar, S., Majumdar, A., and Tien, C.L., (1988), "The Differential Discrete Ordinate Method for Solutions of the Equation of Radiative Transfer", in *ASME Proceedings of the 1988 National Heat Transfer Conference*, Jacobs, H.R. (ed.), pp.179-186, American Society of Mechanical Engineers, New York.

Lee, H., and Buckius, R.O., (1986), "Combined Mode Heat Transfer Analysis Utilizing Radiation Scaling", *Journal of Heat Transfer*, v.108, n.3, pp.626-632.

Lee, H., Chikh, S., and Ma, Y., (1988), "Full Thermal Development of Radiatively Participating Media in Poiseuille Flow", presented at the AIAA Thermophysics, Plasmadynamics, and Lasers Conference, June 27-29, San Antonio, Texas.

Lee, J.S., and Humphrey, J.A.C., (1986), "Radiative-Convective Heat Transfer in Dilute Particle-Laden Channel Flows", *PhysicoChemical Hydrodynamics*, v.7, n.5/6, pp.325-351.

Lewis, E.E. and Miller, W.F. jr., (1984), *Computational Methods of Neutron Transport*, John Wiley & Sons, New York.

Menguc, M.P., and Viskanta, R., (1985a), "Radiative Transfer in Three-Dimensional Rectangular Enclosures Containing Inhomogeneous, Anisotropically Scattering Media", *Journal of Quantitative Spectroscopy and Radiative Transfer*, v.33, n.6, pp.533-549.

Menguc, M.P., and Viskanta, R., (1985b), "On the Radiative Properties of Polydispersions: A Simplified Approach", *Combustion Science and Technology*, v.44, pp.143-159.

Menguc, M.P., and Viskanta, R., (1986), "Radiative Transfer in Axisymmetric, Finite Cylindrical Enclosures", *Journal of Heat Transfer*, v.108, pp.271-276.

Modest, M.F., (1981), "Radiative Heat Transfer in a Plane-Layer of Non-Gray Particles and Molecular Gases", *Journal of Quantitative Spectroscopy and Radiative Transfer*, v.26, n.6, pp.523-533.

Ozisik, M.N., (1973), *Radiative Transfer*, John Wiley & Sons, New York.

Panton, R.L., (1984), *Incompressible Flow*, John Wiley & Sons, New York.

Qian, R., Huang, W., Xu, Y., and Liu, D., (1987), "Experimental Research of Radiative Heat Transfer in Fluidized Beds", *International Journal of Heat and Mass Transfer*, v.30, n.5, pp.827-831.

Ratzel, A.C., and Howell, J.R., (1982), "Two-Dimensional Energy Transfer in Radiatively Participating Media with Conduction by the P-N Approximation", *Proceedings of the Seventh International Heat Transfer Conference*, v.R14, pp.535-540.

Razzaque, M.M., Howell, J.R., and Klein, D.E., (1984), "Coupled Radiative and Conductive Heat Transfer in a Two-Dimensional Rectangular Enclosure with Gray Participating Media Using Finite Elements", *Journal of Heat Transfer*, v.106, n.3, pp.613-619.

Roberson, J.A. and Crowe, C.T., (1975), *Engineering Fluid Mechanics*, Houghton Mifflin, Boston.

Ryhmimg, I.L., (1966), "Radiative Transfer Between Two Concentric Spheres Separated by an Absorbing and Emitting Gas", *International Journal of Heat and Mass Transfer*, v.9, pp.315-324.

Self, S.A., (1987), "Comments on 'Rigorous Bounds on the Radiative Interaction Between Real Gases and Scattering Particles' by D.G. Goodwin and J.L. Ebert", *Journal of Quantitative Spectroscopy and Radiative Transfer*, v.37, n.5, pp.513-514.

Siegel, R. and Howell, J.R., (1981), *Thermal Radiation Heat Transfer*, 2nd ed., Hemisphere Publishing Corporation, Washington D.C.

Sharma, M.P., and Crowe, C.T., (1979), "A Computer Mathematical Model for Gas-Particle Two-Phase Flows", Presented at the Multi-Phase Flow and Heat Transfer Symposium-Workshop, Miami Beach, Florida, April 16-18; also in Veziroglu, T.N. (ed.) *Multiphase Transport - Fundamentals, Reactor Safety, Applications*, Hemisphere Publishing Corp., Washington, D.C.

Skycopec, R.D., and Buckius, R.O., (1984), "Total Hemispherical Emittances for CO₂ or H₂O Including Particulate Scattering", *International Journal of Heat and Mass Transfer*, v.27, n.1, pp.1-12.

Skycopec, R.D., and Buckius, R.O., (1987), "Comments on 'Rigorous Bounds on the Radiative Interaction Between Real Gases and Scattering Particles' by D.G. Goodwin and J.L. Ebert", *Journal of Quantitative Spectroscopy and Radiative Transfer*, v.37, n.5, pp.509-511.

Sirignano, W.A., (1983), "Fuel Droplet Vaporization and Spray Combustion Theory", *Progress in Energy and Combustion Science*, v.9, pp.291-322.

Smith, P.J., Fletcher, T.H., and Smoot, L.D., (1981), "Model for Pulverized Coal-Fired Reactors", *Proceedings of the Eighteenth Symposium (International) on Combustion*, The Combustion Institute, pp. 1285-1293.

Smith, P.J., Fletcher, T.H., and Smoot, L.D., (1985), *Prediction and Measurement of Entrained Flow Coal Gasification Processes; Volume II, User's Manual for a Computer Program for 2-Dimensional Coal Gasification or Combustion*, final report for US/DOE contract no. DE-AC21-81MC16518, 28 February, 1985.

Smith, T.F., Al-Turki, A.M., Byun, K., and Kim, T.K., (1987), "Radiative and Conductive Transfer for a Gas/Soot Mixture Between Diffuse Parallel Plates", *Journal of Thermophysics and Heat Transfer*, v.1, pp.50-55.

Soo, S.L., (1967), *Fluid Dynamics of Multiphase Systems*, Blaisdell Publishing Company, Waltham, Massachusetts.

Soo, S.L., (1989), *Particulates and Continuum: Multiphase Fluid Dynamics*, Hemisphere Publishing Corporation, Washington, D.C.

- Tabanfar, S., and Modest, M.F., (1983), "Radiative Heat Transfer in a Cylindrical Mixture of Non-Gray Particulates and Molecular Gases", *Journal of Quantitative Spectroscopy and Radiative Transfer*, v.30, n.6, pp.555-570.
- Tabanfar, S., and Modest, M.F., (1987), "Combined Radiation and Convection in Absorbing, Emitting, Nongray Gas-Particulate Tube Flow", *Journal of Heat Transfer*, v.109, n.2, pp.478-484.
- Tien, C.L., (1961), "Heat Transfer by a Turbulently Flowing Fluid-Solids Mixture in a Pipe", *Journal of Heat Transfer*, v.83, n.2, pp.183-188.
- Truelove, J.S., (1987), "Discrete Ordinate Solutions for the Radiation Transport Equation", *Journal of Heat Transfer*, v.109, n.4, pp.1048-1051, November.
- Truelove, J.S., (1988), "Three Dimensional Radiation in Absorbing, Emitting, Scattering Media Using the Discrete Ordinates Approximation", *Journal of Quantitative Spectroscopy and Radiative Transfer*, v.39, n.1, pp.27-31, January.
- Tsai, J.H., Ozisik, M.N., and Santarelli, F., (1989), "Radiation in Spherical Symmetry with Anisotropic Scattering and Variable Properties", *Journal of Quantitative Spectroscopy and Radiative Transfer*, v.42, n.3, pp.187-199.
- Viskanta, R. and Crosbie, A.L., (1967), "Radiative Transfer Through a Spherical Shell of an Absorbing, Emitting Gray Medium", *Journal of Quantitative Spectroscopy and Radiative Transfer*, v.7, pp.871-889.
- Viskanta, R., and Menguc, M.P., (1987), "Radiation Heat Transfer in Combustion Systems", *Progress in Energy and Combustion Science*, v.13, pp.97-160.
- Viskanta, R., and Merriam, R.L., (1968), "Heat Transfer by Combined Conduction and Radiation Between Concentric Spheres Separated by Radiating Medium", *Journal of Heat Transfer*, v.90, pp.248-256.
- Yener, Y., and Ozisik, M.N., (1986), "Simultaneous Radiation and Forced Convection in Thermally Developing Turbulent Flow Through a Parallel-Plate Channel", *Journal of Heat Transfer*, v.108, n.4, pp.985-988.
- Yucel, A., Acharya, S., and Williams, M.L., (1988), "Combined Natural Convection and Radiation in a Square Enclosure", in Jacobs, H.R. (ed.), *ASME Proceedings of the 1988 National Heat Transfer Conference*, ASME HTD-96, v.1, pp.209-218.
- Yucel, A., and Williams, M.L., (1987), "Heat Transfer by Combined Conduction and Radiation in Axisymmetric Enclosures", *Journal of Thermophysics and Heat Transfer*, v.1, pp.301-306.
- Yucel, A. and Williams, M.L., (1988), "Interaction of Conduction and Radiation in Cylindrical Geometry without Azimuthal Symmetry", in *ASME Proceedings of the 1988 National Heat Transfer Conference*, Jacobs, H.R. (ed.), pp.281-290, American Society of Mechanical Engineers, New York.

APPENDIX A - SPATIALLY AXISYMMETRIC DIRECTIONAL COORDINATE SYSTEM

INTRODUCTION

The objective of this appendix is to demonstrate the form of the radiative pathlength derivative, dI/ds , in the coordinate system designated Spatially Axisymmetric Directional, for both spatially spherical and spatially cylindrical coordinates.

The Spatially Axisymmetric Directional coordinate system, illustrated in fig.A.1 for spatially spherical coordinates, is a spatial-directional coordinate system based on a polar axis which is normal to the spatial plane of symmetry, and is therefore perpendicular to the spatial location vector. This is different from the spatial-directional coordinate system generally used to express radiative intensity (see Lewis and Miller, 1984), in which the polar vector is an extension of the radial spatial component vector in spatially spherical and cylindrical coordinate systems. In the traditional coordinate system, differential paths ds normal to the plane of symmetry, at the plane of symmetry, are not functions of one directional coordinate. This leads to difficulty in expressing boundary conditions for the directional variable partial derivatives, which appear in the radiative transfer equation in curvilinear spatial coordinates.

The approach taken in this appendix is to derive the pathlength derivative in spatially spherical coordinates, and derive the spatially cylindrical expression from that result.

Figure A.1 - Spatially axisymmetric directional coordinate system for representation of radiation intensity in spatially spherical coordinates

SPATIALLY SPHERICAL COORDINATES

The Spatially Axisymmetric Directional coordinate system for spatial spherical coordinates is shown in fig.A.1. The spatial location is defined by r, ϕ , and ψ , where ψ is the rotation out of the x-y plane (plane 1), about the x axis, out to the plane of symmetry (plane 2), and r and ϕ define the location in the plane of symmetry. The direction of the radiation intensity at the spatial location is defined by a second spherical coordinate system with its origin at the spatial location. The polar axis is normal to the axisymmetric plane (plane 2). The corresponding azimuthal angle lies in a plane parallel to the plane of symmetry. The azimuthal angle is the rotation about the polar axis defined by γ ; the polar angle α is defined in a plane (plane 3) which is hinged on the polar axis and rotated through γ away from the radial vector extension (the arbitrarily defined γ branch cut); directions with $\alpha=\pi/2$ and any γ lie in the plane of symmetry (plane 2).

Using the coordinate system of fig.A.1, we may expand the intensity pathlength derivative into scalar form:

$$\frac{dI}{ds} = \frac{dr}{ds} \frac{\partial I}{\partial r} + \frac{d\phi}{ds} \frac{\partial I}{\partial \phi} + \frac{d\psi}{ds} \frac{\partial I}{\partial \psi} + \frac{d\alpha}{ds} \frac{\partial I}{\partial \alpha} + \frac{d\gamma}{ds} \frac{\partial I}{\partial \gamma} \quad (A.1)$$

where the spatial coordinate coefficients may be derived from projections of the path length element ds onto the radial, binormal, and normal unit vectors (for, respectively, the r , ϕ , and ψ coefficients):

$$\frac{dr}{ds} = \sin \alpha \cos \gamma \quad (A.2a)$$

$$\frac{d\phi}{ds} = \frac{1}{r} \sin \alpha \sin \gamma \quad (\text{A.2b})$$

$$\frac{d\psi}{ds} = \frac{\cos \alpha}{r \sin \phi} \quad (\text{A.2c})$$

The directional coordinate coefficients are derived by noting the correlation between the differentials of the spatial and directional angles. If the change in a directional angle with the differential path ds lies in a plane parallel to the plane in which the change in a spatial angle lies, then these two differential angles may be related as shown in fig.A.2 (see also Ozisik (1973), p.262). Since changes in γ are always in a plane parallel to the plane of symmetry, which contains changes in the spatial angle ϕ , through the identity that the sum of interior angles of a triangle sum to π , it is easily shown:

$$d\gamma = -d\phi \quad (\text{A.3a})$$

and therefore:

$$\frac{d\gamma}{ds} = -\frac{1}{r} \sin \alpha \sin \gamma \quad (\text{A.3b})$$

The change in polar angle $d\alpha$ may be related to the change in the spatial angle out of the plane of symmetry $d\psi$ by projecting $d\psi$ into the plane of $d\alpha$, as shown in fig.A.3. Figure A.3 shows the spatial plane of symmetry in the plane of the page; note that the vertical axis is y'' , as defined in fig.A.1. By the definition of the polar axis in the Spatially Axisymmetric Directional coordinate system, the plane of $d\alpha$ must be normal to the plane of symmetry, rotated through an angle γ from the radial vector's

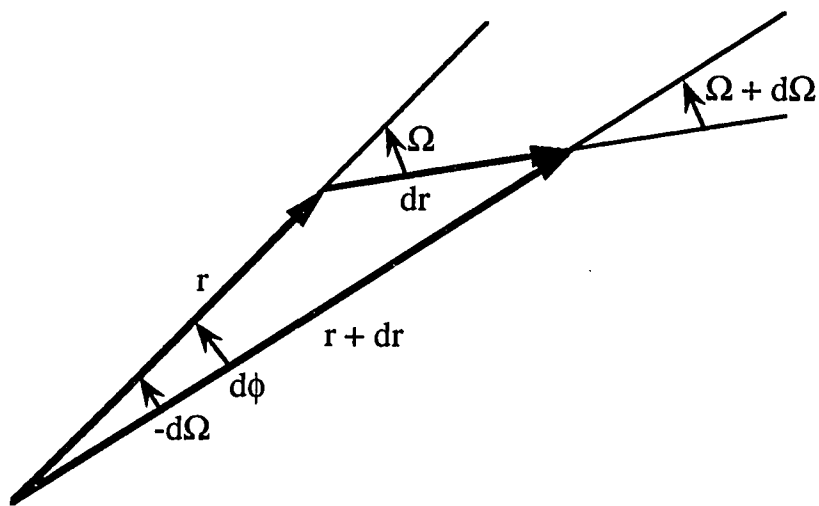


Figure A.2 - Correlation between differential spatial angles and differential directional angles - first kind

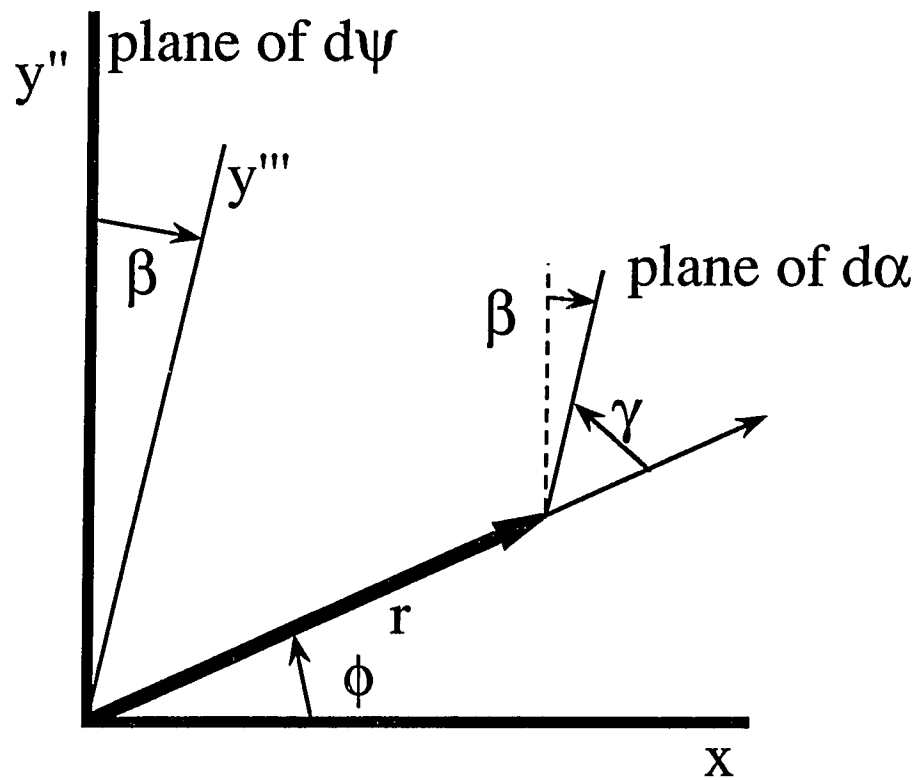


Figure A.3 - Projection of spatial azimuthal differential angle ($d\psi$)
on plane of directional polar differential angle ($d\alpha$)

extension. If the plane of $d\psi$ is projected onto the instantaneous plane of $d\alpha$, in which $d\psi$ is transformed to $d\psi_p$, then the analytical relationship may be expressed:

$$\frac{d\alpha}{ds} = \frac{d\psi}{ds} \frac{d\psi_p}{d\psi} \frac{d\alpha}{d\psi_p} \quad (\text{A.4a})$$

in which:

$$\frac{d\psi_p}{d\psi} = \cos \beta \quad (\text{A.4b})$$

where:

$$\beta = \frac{\pi}{2} - \phi - \gamma \quad (\text{A.4c})$$

Figure A.4 shows both $d\psi_p$ and $d\alpha$ in the plane of the page, where the vertical axis is y''' as defined by fig.A.3. Solving the angles of the triangle results in:

$$d\alpha = d\psi_p \quad (\text{A.4d})$$

By applying trigonometric identities, the result is achieved:

$$\frac{d\alpha}{ds} = \frac{\cos \alpha}{r \sin \phi} (\sin \gamma \cos \phi + \cos \gamma \sin \phi) \quad (\text{A.4e})$$

Substituting eqs.A.2, 3b, and 4e into eq.A.1, and applying conservative form, gives the final result for spatially spherical coordinates:

$$\begin{aligned} \frac{dI}{ds} = & \frac{1}{r^2} \sin \alpha \cos \gamma \frac{\partial}{\partial r} (Ir^2) + \frac{\sin \alpha \sin \gamma}{r \sin \phi} \frac{\partial}{\partial \phi} (I \sin \phi) + \frac{\cos \alpha}{r \sin \phi} \frac{\partial I}{\partial \psi} \\ & + \frac{1}{r} \left(\cos \alpha + \frac{\sin \gamma}{\tan \phi} \right) \frac{\partial}{\partial \alpha} (I \cos \alpha) - \frac{\sin \alpha}{r} \frac{\partial}{\partial \gamma} (I \sin \gamma) \end{aligned} \quad (\text{A.5})$$

which reduces properly to simple form (only I in the derivatives). In axisymmetric

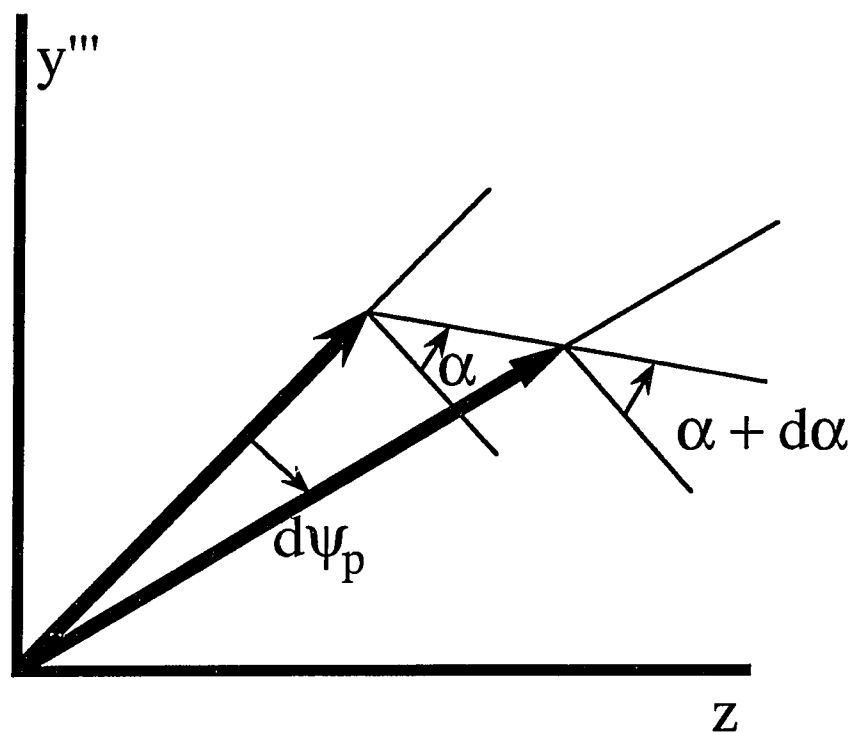


Figure A.4 - Correlation between differential spatial angles and differential directional angles - second kind

problems, $\partial I / \partial \psi = 0$.

SPATIALLY CYLINDRICAL COORDINATES

The coordinate system for spatially cylindrical coordinates is shown in fig.A.5.

In this coordinate system, the intensity pathlength derivative is:

$$\frac{dI}{ds} = \frac{dr}{ds} \frac{\partial I}{\partial r} + \frac{dx}{ds} \frac{\partial I}{\partial x} + \frac{d\psi}{ds} \frac{\partial I}{\partial \psi} + \frac{d\alpha}{ds} \frac{\partial I}{\partial \alpha} + \frac{d\gamma}{ds} \frac{\partial I}{\partial \gamma} \quad (\text{A.6})$$

and the spatial derivative coefficients may be seen from fig.A.5 to be:

$$\frac{dr}{ds} = \sin \alpha \cos \gamma \quad (\text{A.7a})$$

$$\frac{dx}{ds} = -\sin \alpha \sin \gamma \quad (\text{A.7b})$$

$$\frac{d\psi}{ds} = \frac{\cos \alpha}{r} \quad (\text{A.7c})$$

The directional derivative coefficients in the spatially spherical coordinates case resulted from the new direction of I with respect to the directional coordinate system as defined with its origin in a new location, following the spatial relocation ds . In other words, since the location had moved by ds , the directional coordinate system was reoriented based on a repositioned polar axis and azimuthal branch cut, and the direction coordinates as defined by this new directional coordinate system were different than the directional coordinates defined by the old directional coordinate system, before the spatial relocation ds . Put more succinctly, the directional derivative coefficients are the directional bookkeeping resulting from a spatial move ds . The absolute direction of intensity remained constant throughout the spatial move ds . In spatially cylindrical coordinates, because γ is defined with respect to the radial vector, and because the

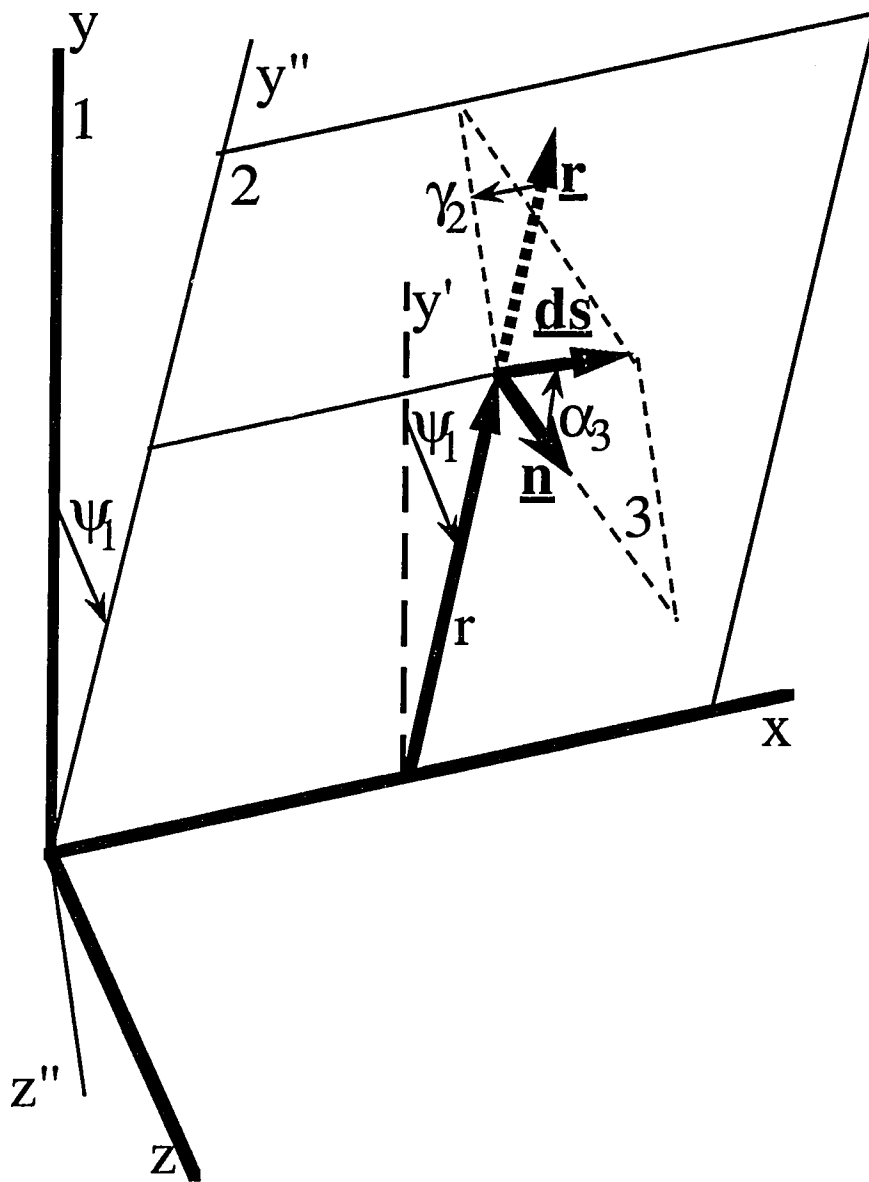


Figure A.5 - Spatially axisymmetric directional coordinate system for representation of radiation intensity in spatially cylindrical coordinates

radial vector never changes its orientation with respect to the plane in which γ is defined, for a constant absolute direction and a spatial change ds :

$$\frac{d\psi}{ds} = 0 \quad (\text{A.8})$$

This can be shown mechanically by starting from the spatially spherical directional derivatives and imposing $d\phi=0$, with the result $d\gamma=0$.

For α , the construction is similar to that for spatially spherical coordinates, with the exception that $\beta=\gamma$, resulting in:

$$\frac{d\alpha}{ds} = \frac{1}{r} \cos \alpha \cos \gamma \quad (\text{A.9})$$

which could be shown mechanically by starting from the spatially spherical directional derivatives and imposing $\phi=\pi/2$.

Combining eqs.A.6, 7, 8, and 9 and putting the result in conservative form:

$$\begin{aligned} \frac{dI}{ds} = & \frac{1}{r} \sin \alpha \cos \gamma \frac{\partial}{\partial r} (Ir) - \sin \alpha \sin \gamma \frac{\partial I}{\partial x} \\ & + \frac{1}{r} \cos \alpha \frac{\partial I}{\partial \psi} + \frac{1}{r} \cos \gamma \frac{\partial}{\partial \alpha} (I \cos \alpha) \end{aligned} \quad (\text{A.10})$$

which reduces properly to simple form. In axisymmetric problems, $\partial I / \partial \psi = 0$.

APPENDIX B - INTERPHASE HEAT TRANSFER BY COMBINED RADIATION, CONDUCTION, AND CONVECTION

INTRODUCTION

Although heat transfer by convection from a sphere in motion through an infinite medium has been extensively addressed in the literature, there has been little attention given to the case in which radiation heat transfer through participation of the medium is also significant. In a medium which is both radiatively participating and conducting, the existence of these two modes of heat transfer gives rise to temperature profiles distinct from those corresponding to either radiation, conduction, or convection acting alone. As a result, it is necessary to perform a combined analysis to determine the heat flux from a sphere in such a medium, and it may not be accurate to simply add heat flux correlations taken from independent analyses of either heat transfer mode.

Correlations for heat transfer from a sphere in motion in non-radiatively participating media are derived by considering the sphere to be a constant temperature inner surface in a spherical annulus, where the outer surface is expanded to infinity and is also held at a constant temperature. In the case of zero velocity, the analysis reduces to solution of a second order differential equation. In the present radiatively participating case, a spherical annulus is similarly addressed. However, radiation heat transfer terms in the energy equation are governed by the continuous radiation intensity, which is the solution of the radiative transfer equation. Therefore, in the present analysis, it is necessary to solve a coupled formulation for the temperature and the radiation intensity in the thermal boundary layer around the particle in order to express the overall heat transfer between the particle and the continuous medium. The results of this analysis, either in graphical or correlation equation form, may be used to express heat transfer between a dispersed spherical phase in motion through a continuous

phase, developed in a manner analogous to the widely used correlations for the special case of a radiatively non-participating medium (Nusselt number).

One-dimensional heat transfer by radiation alone in a spherical annulus has been solved by a variety of methods. Ryhming (1966) and Viskanta and Crosbie (1967) presented coupled temperature and intensity solutions using an exponential integral solution for the radiative transfer, set out by Kuznetsov in a 1951 Russian language paper. Viskanta and Merriam (1968) included conduction in the medium in a similar analysis. Bayazitoglu and Suryanarayana (1989) developed closed form solutions to the pure radiation problem using the spherical harmonics method for the radiative transfer, as developed in Bayazitoglu and Higenyi (1979). Tsai, et al. (1989) addressed the radiative transfer for a given temperature profile using the discrete ordinates method. These analyses are all one-dimensional in that there is only radial variation in the temperature, and are thus spatially radially symmetric. As a result, the variation of intensity with direction may be expressed in a single angular coordinate, being directionally radially symmetric as well. The present problem, involving flow over a sphere, is spatially two-dimensional and axisymmetric. The resulting radiative transfer expression must involve two angular coordinates. Therefore, none of the previous solutions for radiative transfer in a spherical annulus apply directly to the present problem.

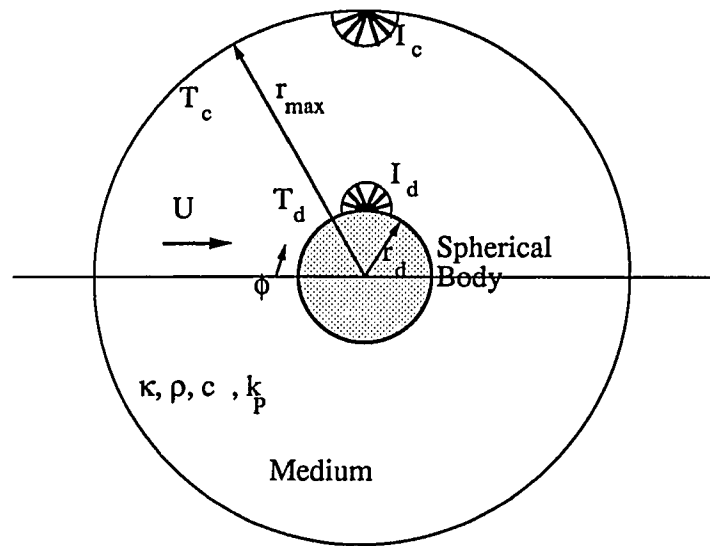


Figure B.1 - Spherical body in motion through a gray, absorbing, emitting, conducting medium

ANALYSIS

Governing Equations

The geometry of the problem is illustrated in fig.B.1 as an axisymmetric slice of a spherical annulus. The energy equation in this region may be written:

$$\rho c_p \frac{DT}{Dt} + \nabla \cdot \mathbf{q}^C + \nabla \cdot \mathbf{q}^R = 0 \quad (\text{B.1})$$

Assuming steady state, constant properties, an index of refraction of unity, Kirchoff's law, and making substitutions for each term, we have:

$$\rho c_p \vec{\nabla} \cdot \nabla T - k \nabla^2 T + 4\kappa \sigma T^4 - \kappa \int_0^\pi \int_0^{2\pi} I \sin \alpha \, d\gamma \, d\alpha = 0 \quad (\text{B.2})$$

where the radiation intensity I is integrated over a directional element of solid angle. It is assumed that the medium is gray, with radiation intensity not varying with radiation frequency, so that κ is a spectrally averaged quantity. The velocity field is assumed to be known. Equation B.2 may be written in scalar form in r and ϕ in the normal way.

It is assumed that the medium is non-scattering. A possible application for the results of this analysis is as an expression of the interphase heat transfer term in a particle or droplet flow. In such a flow, the principal scattering mode is scattering from the particles or droplets themselves. The present problem, as applied to such a flow, represents only a single particle or droplet, surrounded by the continuous medium in pure (non-particle laden) form. Therefore, scattering has been neglected for the present analysis of interphase heat transfer. This might be regarded as an inner, single-particle problem, where the outer, multi-particle problem would involve both interparticle scattering as well as the inner problem heat transfer results. The non-scattering, gray,

constant properties form of the radiative transfer equation, assuming Kirchoff's law, and with an index of refraction of unity is:

$$\frac{dI}{ds} + \kappa I = \kappa \frac{\sigma}{\pi} T^4 \quad (B.3)$$

where the radiation intensity I and the differential path length ds are functions of both spatial variables and the two angular variables necessary to define the direction.

Intensity is therefore a four-dimensional quantity in this problem.

Coordinate System

For one-dimensional problems, a suitable and frequently used coordinate system is based on a polar axis which is a unit extension of the radial vector. The two components of direction are then the polar angle, rotated out from the radial extension, and the azimuthal angle, rotated about the radial extension. This system is advantageous for one-dimensional problems because these problems are symmetric in the azimuthal angle, and there is a zero-slope boundary condition at each end of the polar angle excursion. However, neither of these advantages apply to the two-dimensional problem considered here. Since the temperature varies with ϕ , the radiation intensity cannot be symmetric with an azimuthal angle about the radial extension. Further, for this (spatially) two-dimensional problem, the symmetric zero-slope boundary condition for the polar angle holds only in special cases. Therefore, the coordinate system established in Appendix A is applied, using the expression for dI/ds from eq.A.5.

Boundary Conditions

The sphere is assumed to have a constant surface temperature, which is known,

and the medium bulk temperature outside the thermal boundary layer is also assumed to be known. Thus:

$$T(r_d, \phi) = T_d \quad (\text{B.4a})$$

$$T(r_{\max}, \phi) = T_c \quad (\text{B.4b})$$

where d denotes the dispersed phase (the droplet or particle), c denotes the continuous phase (the medium), and r_{\max} is the computational outer boundary. Due to the axisymmetry of the problem, leading and trailing edge boundary conditions may be written:

$$\frac{\partial T}{\partial \phi}(r, 0) = 0 \quad (\text{B.5a})$$

$$\frac{\partial T}{\partial \phi}(r, \frac{\pi}{2}) = 0 \quad (\text{B.5b})$$

The radiation intensity at either boundary facing into the annulus is assumed to be known. Here a boundary condition is used at the inner surface which is consistent with diffuse emission and reflection from the solid surface of a particle:

$$I(r_d, \phi, \alpha, \gamma_{\text{out}}) = \epsilon_d \frac{\sigma}{\pi} T_d^4 + (1 - \epsilon_d) \frac{1}{\pi} \int_{\frac{\pi}{2}}^{\frac{3\pi}{2}} \int_0^{\pi} I(r_d, \phi, \alpha, \gamma) \sin^2 \alpha \cos \gamma \, d\alpha \, d\gamma \quad (\text{B.6a})$$

where γ_{out} on the left hand side denotes that I_d is given only for those γ 's facing away from the sphere's surface, and the integration range for γ on the right hand side includes only those γ 's facing in towards the surface. As alternatives to eq.B.6a, a

specular surface reflection or any other non-diffuse surface intensity distribution could be substituted. At the outer boundary, a black, diffuse boundary condition is assumed:

$$I(r_{\max}, \phi, \alpha, \gamma_{\text{in}}) = I_c = \frac{\sigma}{\pi} T_c^4 \quad (\text{B.6b})$$

A leading edge boundary condition also applies to the radiation intensity:

$$\frac{\partial I}{\partial \phi}(r, 0, \alpha, \gamma) = 0 \quad (\text{B.7})$$

The radiation intensity is symmetric in α , so only half of the range $0 < \alpha < \pi/2$ is considered. Normal to the plane of symmetry:

$$\frac{\partial I}{\partial \alpha}(r, \phi, \frac{\pi}{2}, \gamma) = 0 \quad (\text{B.8})$$

The radiation intensity is continuous in γ . Parallel to the axisymmetric plane, for all α :

$$I(r, \phi, \alpha, 0) = I(r, \phi, \alpha, 2\pi) \quad (\text{B.9})$$

Numerical Procedure

To summarize, the problem is a non-linear, second order, two-dimensional energy equation coupled to a linear, first order, four-dimensional radiative transfer equation. The overall numerical scheme is to estimate temperature, solve the radiative transfer equation for the given temperature, and use the resulting intensity to solve a linearized form of the energy equation. The temperature solution is then compared to the temperature estimate, a new estimate is formed by over-relaxing the estimation error, and the loop is repeated until convergence is achieved. The energy equation is multiplied by an element of volume, $2\pi r^2 \sin \phi \, d\phi \, dr$, and integrated between $r_{j-1/2}$ and

$r_{j+1/2}$, and between $\phi_{k-1/2}$ and $\phi_{k+1/2}$, to reach the final form of the finite difference equation. A variable mesh is used in r to provide very fine spacing near the sphere's surface, and provide the ability to expand to very large values for the outer boundary.

A uniform mesh is used in the ϕ direction. The energy equation is block tridiagonal and could have been solved with a specialized block matrix version of the Thomas algorithm; however, since iteration is already required for the linearized terms, the more rapid, iterative solution method of alternating direction implicit (ADI, see Anderson, et al (1984), p.136) is used to solve the energy equation in the r and ϕ directions.

For the numerical simulation of the radiative transfer equation, the conservative form for the path length derivative is used, eq.A.5. The conservative form is generally necessary for numerical stability in spherical coordinate systems, although it is not mathematically necessary in this case. Equation A.5 is multiplied by an element of volume and solid angle, $2\pi r^2 \sin \phi \, d\phi \, dr \sin \alpha \, d\alpha \, d\gamma$, and integrated over Δr , $\Delta\phi$, w_ϕ , and w_m . The final form of the difference equation is:

$$\begin{aligned}
 & 4\pi \sin \alpha_\ell \cos \gamma_m \sin \delta\phi_k \sin \phi_k w_\ell w_m \left[I_{j+1/2} r_{j+1/2}^2 - I_{j-1/2} r_{j-1/2}^2 \right] \\
 & + \pi \sin \alpha_\ell \sin \gamma_m \delta r_j^2 w_\ell w_m \left[I_{k+1/2} \sin \phi_{k+1/2} - I_{k-1/2} \sin \phi_{k-1/2} \right] \\
 & + 2\pi \sin \delta\phi_k \delta r_j^2 w_m (\cos \gamma_m \sin \phi_k + \sin \gamma_m \cos \phi_k) \left[I_{\ell+1/2} A_{\ell+1/2} - I_{\ell-1/2} A_{\ell-1/2} \right] \\
 & + 2\pi \sin \alpha_\ell \sin \delta\phi_k \sin \phi_k \delta r_j^2 w_\ell \left[I_{m+1/2} \Gamma_{m+1/2} - I_{m-1/2} \Gamma_{m-1/2} \right] \\
 & + I \kappa \frac{4\pi}{3} \delta r_j^3 \sin \delta\phi_k \sin \phi_k w_\ell w_m \\
 & = T^4 \kappa \frac{4\sigma}{3} \delta r_j^3 \sin \delta\phi_k \sin \phi_k w_\ell w_m
 \end{aligned} \tag{B.10}$$

where:

$$\begin{aligned}\delta\phi_k &= \frac{1}{2}(\phi_{k+1/2} - \phi_{k-1/2}) \\ \delta r_j^2 &= r_{j+1/2}^2 - r_{j-1/2}^2\end{aligned}$$

Equation B.10 uses the linear cell-center relations:

$$I_j = \frac{1}{2}(I_{j+1/2} + I_{j-1/2}) \quad (\text{B.11a})$$

$$I_k = \frac{1}{2}(I_{k+1/2} + I_{k-1/2}) \quad (\text{B.11b})$$

$$I_l = \frac{1}{2}(I_{l+1/2} + I_{l-1/2}) \quad (\text{B.11c})$$

$$I_m = \frac{1}{2}(I_{m+1/2} + I_{m-1/2}) \quad (\text{B.11d})$$

These are termed the "diamond difference" relations by Lewis and Miller (1984). In eq.B.10, the coefficients A and Γ replace the analytical coefficients of eq.A.5 as a means of satisfying the condition that for constant I , $dI/ds=0$. This condition is non-trivial because while the derivatives of the coefficients inside the partials in eq.A.5 cancel in the sum over all four terms, the same is not necessarily true for the finite difference form of the derivatives. In order for the condition $dI/ds=0$ for constant I to hold for the discretized form, it can be shown that the spatial and directional meshes must be uniform. Rather than allow this restriction and loose the α quadrature and the variable r mesh, the coefficients in the discretized form of the equation are altered specifically to satisfy the condition $dI/ds=0$ for constant I . This condition is discussed more fully by Lewis and Miller (1984). Applying the condition directly to solve for the discrete coefficients gives the recursion equations:

$$A_{\ell+1/2} - A_{\ell-1/2} = -w_\ell \sin \alpha_\ell \quad (\text{B.12a})$$

$$\Gamma_{m+1/2} - \Gamma_{m-1/2} = -w_m \cos \gamma_m \quad (\text{B.12b})$$

By analogy to the analytical coefficients, with $\alpha_{L+1/2}=\pi/2$ and $\gamma_{1/2}=0$, $A_{L+1/2}=0$ and

$\Gamma_{1/2}=0$ are taken as starting values for the recursions.

RESULTS AND DISCUSSION

In order to determine the parameters important to the solution, the energy equation is written in non-dimensional form, substituting dI/ds for the radiation terms:

$$\begin{aligned} & \frac{1}{\text{Pl}} \int_0^{2\pi} \int_0^\pi \frac{1}{\zeta^2} \sin \alpha \cos \gamma \frac{\partial}{\partial \zeta} (\zeta^2 \Phi) \sin \alpha \, d\alpha \, d\gamma \\ & + \frac{1}{\text{Pl}} \int_0^{2\pi} \int_0^\pi \frac{\sin \alpha \sin \gamma}{\zeta \sin \phi} \frac{\partial}{\partial \phi} (\sin \phi \Phi) \sin \alpha \, d\alpha \, d\gamma \\ & + \frac{1}{\text{Pl}} \int_0^{2\pi} \int_0^\pi \frac{1}{\zeta} \left(\cos \gamma + \frac{\sin \gamma}{\tan \phi} \right) \frac{\partial}{\partial \alpha} (\cos \alpha \Phi) \sin \alpha \, d\alpha \, d\gamma \\ & - \frac{1}{\text{Pl}} \int_0^{2\pi} \int_0^\pi \frac{\sin \alpha}{\zeta} \frac{\partial}{\partial \gamma} (\sin \gamma \Phi) \sin \alpha \, d\alpha \, d\gamma \\ & - \left[\frac{1}{\zeta^2} \frac{\partial}{\partial \zeta} \left(\zeta^2 \frac{\partial \Theta}{\partial \zeta} \right) + \frac{1}{\zeta^2 \sin \phi} \frac{\partial}{\partial \phi} \left(\sin \phi \frac{\partial \Theta}{\partial \phi} \right) \right] \\ & + \frac{\text{Pe}}{2} \left[\left(\frac{v_r}{U} \right) \frac{\partial \Theta}{\partial \zeta} + \frac{1}{\zeta} \left(\frac{v_\phi}{U} \right) \frac{\partial \Theta}{\partial \phi} \right] = 0 \end{aligned} \quad (\text{B.13})$$

where:

$$\Theta = T/T_d$$

$$\Phi = I/4\sigma T_d^4$$

$$\zeta = r/r_d$$

The first group of four terms in eq.B.13 is the radiation part, the second group is the conduction part, and the third group is the convection part. The importance of the radiation term relative to the conduction term is governed by the Planck number,

$Pl=k/(4r_d\sigma T_d^3)$, and that of the convection term by the Peclet number, $Pe=(2Ur_d\rho c_p)/k$.

Similarly, we may rewrite the radiative transfer equation:

$$\begin{aligned} & \frac{1}{\zeta^2} \sin \alpha \cos \gamma \frac{\partial}{\partial \zeta} \left(\zeta^2 \Phi \right) + \frac{\sin \alpha \sin \gamma}{\zeta \sin \phi} \frac{\partial}{\partial \phi} (\sin \phi \Phi) \\ & + \frac{1}{\zeta} \left(\cos \gamma + \frac{\sin \gamma}{\tan \phi} \right) \frac{\partial}{\partial \alpha} (\cos \alpha \Phi) - \frac{\sin \alpha}{\zeta} \frac{\partial}{\partial \gamma} (\sin \gamma \Phi) \\ & + \Phi (\kappa r_d) = \frac{1}{4\pi} (\kappa r_d) \Theta^4 \end{aligned} \quad (B.14)$$

to illustrate the governing parameter κr_d ; the importance of ϵ_d is indicated by the

boundary conditions. Note that κr_d is the non-dimensionalized radius of the sphere,

rather than any physically meaningful optical thickness, as the region inside r_d is not

part of the medium. Further, due to the nonlinear influence of θ upon Φ , the

temperature ratio T_d/T_c is also a governing parameter. Summarizing, the important

parameters in this problem are Pl , Pe , κr_d , ϵ_d , and T_d/T_c . These are the only parameters

which affect a suitably non-dimensionalized result. The rather large number of controlling parameters, as compared to conduction/convection alone without radiation, is a result of the combined mode nature of the problem. In pure radiation, for instance, it may be possible to non-dimensionalize heat flux in such a way as to remove κr_d from the parameter list. However, with combined modes, this is not justifiable.

Figure B.2 shows temperature profiles near the sphere's surface at $Pe=0$, a very large r_{max} , and a variety of Pl . For Pl large, the energy equation is dominated by conduction, and the temperature profile is the solution of the one-dimensional spherical diffusion equation. For Pl near zero, radiation heat transfer dominates the energy equation. The resulting temperature profile shows a temperature jump at the boundary, as it should for pure radiation. As Pl is varied down towards zero, the temperature profile moves from the conduction solution to the radiation solution, although temperature continuity at the boundary is maintained. The steep gradients near the sphere's surface for moderate Pl dictate a fairly fine radial mesh. The results used for interphase heat transfer in gas/particle flows were generated using a non-uniform radial mesh of 72 points, a uniform spatial angular mesh of 9 points, a quadrature directional polar angular mesh of 4 points (not including $\alpha=\pi/2$, which is calculated as a special point without weight), and a uniform directional azimuthal angular mesh of 16 points. This directional mesh represents the level of discretization necessary to match the results of Viskanta and Crosbie (1967) and of Tsai, et al (1989) within 1%. The radial mesh is finer than required to meet this criterion, in order to track the continuous temperature distribution near the sphere surface, and was chosen to meet 0.1% self convergence. The angular mesh was also chosen for a 0.1% self convergence criterion, as applied to the heat flux results.

An important issue in applying the results of this analysis to interphase heat

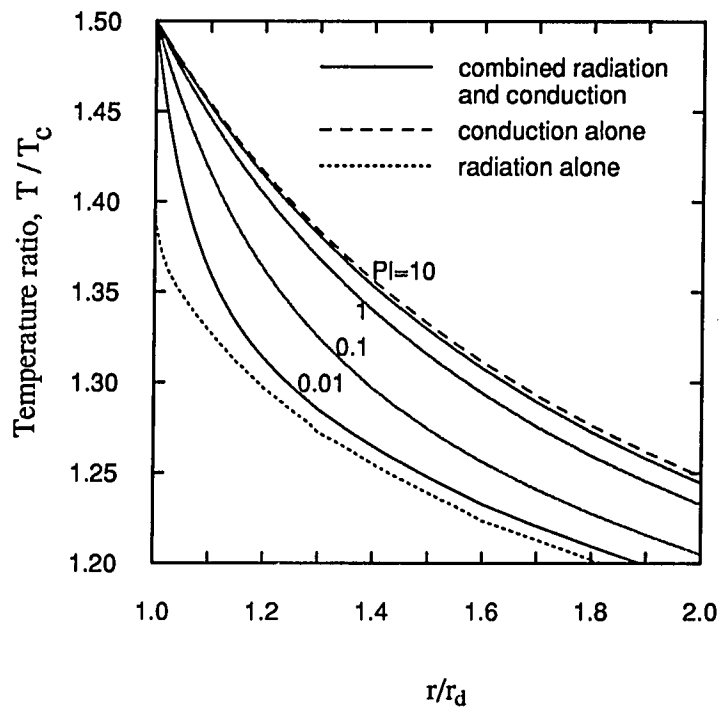


Figure B.2 - Temperature profiles for a black sphere in an infinite medium; for radiation alone, conduction alone, and for combined radiation and conduction, with $T_d/T_c = 1.5$ and $\kappa_c r_d = 1$.

transfer in particle and droplet flow is the extent to which infinite medium results apply to non-infinite particle separation. In fig.3 (main text), the finite radius ratio r_{\max}/r_d for which the heat flux from the sphere's surface is within 5% of the heat flux leaving the surface in an infinite medium, is shown as a function of the non-dimensionalized sphere radius. This is somewhat analogous to a thermal boundary layer thickness. Figure 3 shows that for high Pl, corresponding to a conduction dominated heat transfer, errors due to non-infinite dispersed phase separation will be incurred at a much larger radius ratio than for low Pl, radiation dominated heat transfer. Therefore, use of the present results in the limited context of local heat transfer between a droplet or particle and the proximate gas is at least as accurate as using an infinite-medium Nusselt number in a radiatively non-participating continuous phase. These results were computed for $Pe=0$. Note that for $Pe \neq 0$ there will be an increasing thermal wake, which will have an effect on the critical r_{\max}/r_d .

Pure radiation heat flux is often non-dimensionalized by $\sigma(T_d^4 - T_c^4)$, while conduction/convection results are usually non-dimensionalized by $k(T_d - T_c)/2r_d$. These two non-dimensionalizations are consistent with the approximate magnitudes of each mode of heat transfer, but have little meaning when applied to the opposite mode.

Therefore, choosing to non-dimensionalize by, say, $\sigma(T_d^4 - T_c^4)$ will give rational results for low Pl, radiation dominated cases, but as Pl is increased and the significance of conduction/convection is increased, the non-dimensionalized result grows without bound. A similar effect is obtained for non-dimensionalization of combined mode heat transfer by $k(T_d - T_c)/2r_d$. Therefore, we have normalized our results by using the combined non-dimensionalizing factor $[\sigma(T_d^4 - T_c^4) + k(T_d - T_c)/2r_d]$.

For presentation of heat flux results, results for $Pe=0$ are shown first, varying the parameters Pl , κ_d , and T_d/T_c . Computation of these $Pe=0$ results is simplified by setting variations with ϕ to zero, reducing the size of the problem. These results, for radiation combined with conduction and without convection, could also have been computed using the one-dimensional analysis (one spatial dimension, and correspondingly one directional dimension) of Jones and Bayazitoglu (1990). The following results are given for a different set of non-dimensional parameters and a different non-dimensionalized heat flux than those used in the earlier analysis, in order to provide a basis for extension to $Pe \neq 0$ results. Radiation/conduction results are presented to illustrate the basic variation of the heat flux leaving the sphere's surface with Pl , κ_d , ϵ_d , and T_d/T_c , while the variation with Pe is considered to be an additional effect. This is appropriate for low Pe flow, as would be expected in a dispersed gas/particle flow with low relative phase velocities.

Figure 4 (main text) shows the non-dimensionalized heat flux leaving the surface of a sphere hotter than the surrounding medium for a variety of Pl and T_d/T_c , as a function of κ_d , for $Pe=0$, where the heat flux is given by:

$$q = -k \frac{\partial T(r_d, \phi)}{\partial r} + 2 \int_0^{2\pi} \int_0^{\frac{\pi}{2}} I(r_d, \phi, \alpha, \gamma) \sin^2 \alpha \cos \gamma \, d\alpha \, d\gamma \quad (B.15)$$

For high Pl , the result is dominated by conduction, and approximates the familiar result $Nu=2$. As κ_d increases, radiation begins to have an effect. At low Pl , a radiation dominated case, the pure radiation result of $q/\sigma(T_d^4 - T_c^4)$ vs. κ_d is nearly recovered.

At $Pl=1$, clearly a combined mode case, variation with T_d/T_c is more apparent. With reference to movement from a conduction dominated to a combined mode case, note that while the non-dimensionalized heat flux is reduced, the non-dimensionalizing factor has been altered as well. The perception that the inclusion of radiation effects has reduced the total heat flux is, of course, erroneous.

Figure 4 was computed for a black ($\epsilon_d=1$) sphere. In fig.5 (main text), the reflection coefficient $\rho_d=1-\epsilon_d$ is varied. For low Pl , the effect of ρ_d on the radiation heat flux dominates the total heat flux, especially in surface radiation (low κr_d) dominated regimes. For moderate Pl , in combined mode cases, the effect of ρ_d is less pronounced. For high Pl , the heat flux is dominated by conduction, and the effect of ρ_d is negligible.

As noted previously, the energy equation is decoupled from the momentum equation, and so any descriptive velocity field may be used. In particle or droplet flow, the velocity of the dispersed phase relative to the continuous phase is generally very small. Therefore, the velocity field of Stokes flow is used in the following results (see Panton (1984), p.644):

$$v_r = -\frac{U}{2} \cos \phi \left[\left(\frac{r_d}{r} \right)^3 - 3 \left(\frac{r_d}{r} \right) + 2 \right] \quad (B.16a)$$

$$v_\phi = \frac{U}{4} \sin \phi \left[-\left(\frac{r_d}{r} \right)^3 - 3 \left(\frac{r_d}{r} \right) + 4 \right] \quad (B.16b)$$

This velocity field is valid for Reynolds numbers less than one. However, for slightly

higher Reynolds numbers, the deviation of the velocity field from eqs.B16 due to separation in the wake has only a minor effect on heat transfer.

Figure 6 (main text) shows the effect of low Peclet numbers on combined radiation and convection heat flux from the surface of a black sphere in a gray, non-scattering infinite medium, for hot and cold spheres, respectively. Also shown is the convection-only result $Nu=1+(1+Pe)^{1/3}$, which is valid up to a Peclet number of about 10 (Clift, et al, 1978). At high Planck numbers the heat flux is dominated by conduction and convection, and variation with Pe is similar to variation for convection alone. At low Pl, the radiation terms in eq.B.13 dominate the conduction and convection, and the effect of Pe is insignificant. Presumably, at higher Pe, outside the range of Stokes flow, low Pl cases will show greater variation with Pe. Although the objective of this study has focused on low Pe flow for use in interphase heat transfer in gas/particle flows, the formulation given is quite general, and results for higher Pe could easily be developed.